HOT ISOSTATIC DIFFUSION WELDING OF TITANIUM ALLOYS

A Thesis Submitted to the

Department of Materials and Metallurgical Engineering

Bangladesh University of Engineering and Technology

in partial fulfillment of the requirements

for the

Degree of Master of Science in Engineering (Metallurgical)

by

MOHAMMAD OHIDUL ALAM

Department of Materials and Metallurgical Engineering

Bangladesh University of Engineering and Technology

September 1997

The undersigned examiners appointed by the Committee of Advanced Studies and Research (CASR) hereby recommended to the Department of Materials and Metallurgical Engineering of Bangladesh University of Engineering and Technology (BUET), Dhaka, the acceptance of the thesis entitled "Hot Isostatic Diffusion Welding of Titanium Alloys" submitted by Md. Ohidul Alam, Lecturer, Department of Materials and Metallurgical Engineering, BUET, in partial fulfillment of the requirements for the degree of Master of Science in Engineering (Metallurgical).

1. _____ 10/09/97

Dr. Md. Fakhrul Islam — Chairman
Assistant Professor — (Supervisor)
Department of Materials and Metallurgical Engineering
BUET, Dhaka

2. _____

Head — Member
Department of Materials and Metallurgical Engineering
BUET, Dhaka

3. _____

Professor Dr. Ehsanul Haque — Member
Department of Materials and Metallurgical Engineering
BUET, Dhaka

4. _____

Professor Dr. A. A. Md. Rezaul Haque — Member
Department of Materials and Metallurgical Engineering
BUET, Dhaka

5. _____

Professor Dr. Md. Ibrahim — Member
House No. 31, Road No. 4 — (External)
Dhanmondi R/A, Dhaka-1205

DECLARATION

This is to certify that this research work has been carried out by the author under the supervision of Dr. Md. Fakhrul Islam, Assistant Professor, Department of Materials and Metallurgical Engineering, Bangladesh University of Engineering and Technology (BUET), Dhaka. The results presented in this thesis are to the best of my knowledge, original except where reference is made to the work of others. No part of this thesis has previously been submitted for a degree or qualification at this or any other University.

Countersigned

Supervisor

Signature of the author

ABSTRACT

Studies of microduplex Ti-3Al-2.5V (IMI-325) and Ti-6Al-4V (IMI-318) sheets have shown that the materials have a considerable potential for superplastic deformation at temperatures in the range of 840-880°C and 860-920°C respectively. Diffusion welding of IMI-325 have been carried out at temperatures from 840°C to 880°C and pressures 2.1 MPa to 2.5 MPa for 1 hour with the help of a newly constructed mini hot isostatic pressure furnace. An assessment of the quality of welds produced was made on the basis of metallographic examination. It was found that the welding temperature of 860°C and pressure 2.1MPa for 1 hour had produced sound bond between IMI-325 sheets. Sound weld has also been found between dissimilar IMI-325 and IMI-318 at the condition of 860°C + 2.1 MPa + 1 hr during isostatic diffusion welding. Detailed microstructural examination of this weld revealed that the weld interface did not have any significant microstructural difference from the parent structure. In addition, post heat-treatment has been done for welded samples between IMI-318 and titanium aluminide to eliminate microstructural inhomogenity at the interface.

ACKNOWLEDGEMENTS

The author would like to express his profound indebtedness and sincere gratitude to the thesis supervisor Dr. Md. Fakhrul Islam, Assistant Professor, Department of Materials and Metallurgical Engineering, Bangladesh University of Engineering and Technology (BUET), Dhaka for his guidance, constant advice, encouragement and kind help in carrying out the research work as well as in writing this thesis.

The author also wishes to extend his thanks to the following:-

* Professor Dr. Mohar Ali, Ex-Head and Professor Dr. A. A. M. Razaul Haque, Head of the Department of Materials and Metallurgical Engineering, BUET, for providing the laboratory facilities and their kind inspiration in every steps of the work.

* The academic and technical staff in the Department of Materials and Metallurgical Engineering, BUET, for their willing assistance.

* Dr. Norman Ridley, UK, for providing DW couples otherwise this work would not be possible.

* Dr. A. K. M. Dilder Hossain and Dr. Qumrul Ahsan who helped us to buy inconel tubes from UK.

* His parents and well wishers for their continued inspiration throughout the period of this research work.

CONTENTS

In the Name of
ALLAH
The Most Beneficent
The Most Merciful

INTRODUCTION

Hot Isostatic Pressing (HIP) involves the simultaneous application of an inert gas pressure (usually argon gas) and an elevated temperature in a specially constructed pressure tube. Under this temperature and pressure internal pores or defects within a solid body collapse and the contacting surfaces weld-up. Application of HIP to diffusion welding has been attracting a great deal of interest in recent years.

Diffusion Welding (DW) is a solid state joining process in which the cleaned surfaces to be joined are brought together at an elevated temperature. The application of a moderate pressure, at first, brings the two surfaces into intimate contact by instantaneous microplastic collapse of the surface asperities so creating a planar array of interfacial voids. Creep/superplasticity and stress directed atomic diffusion processes transport atoms to the void surfaces from adjacent areas reducing interfacial void volume[1]. If sufficient time is allowed, then the voids will be removed and an atom to atom bond across the original interface will result. The aim of the diffusion welding is to produce a microstructure in the region of the weld-zone which is indistinguishable from that of the parent materials with no discontinuity in properties across the interface[2].

DW combined with Superplastic Froming(SPF) is now a well established technology for the production of complex structures from α/β titanium sheet alloys. This manufacturing route can lead to both cost and weight savings compared with more conventional forming techniques[1,3,4]. It is thought that the titanium alloy has a considerable potential for SPF at temperatures when they have <50% volume fraction of β phase and the average grain size is less than 10 μm. The potential use of these alloys in gas turbine engine requires their joining both to themselves and to other Ti-alloys. Diffusion welding can also join dissimilar metals with a minimum of metallurgical damage because the process precludes melting and solidification experienced during fusion welding.

A hot isostatic pressure (HIP) furnace has been developed to carry out diffusion welding of titanium alloys. IMI-325 is a new near α titanium alloy and no work has been reported previously for diffusion welding of this alloy. In the present work, the conditions to produce a sound weld between two similar sheets of IMI-325 and two dissimilar alloys of IMI-325 to IMI-318 have been investigated. To select diffusion welding temperature, the alloys have been characterized microstructurally with the help of a newly constructed vertical furnace. Attempt has also been made to eliminate microstructural inhomogenity (diffusion affected third zone) from the previously welded samples of IMI-318 to titanium aluminide.

2: LITERATURE REVIEW

2:1 HOT ISOSTATIC PRESSING (HIP)

2:1:1 Introduction

Hot isostatic pressing (HIP) involves the simultaneous application of gas pressure (usually inert argon gas) and elevated temperature in a specially constructed pressure vessel. Under the required pressure and temperature, asperities between two contacting surfaces collapse and the surfaces weld-up. On an atomic scale, the isostatic pressure arises from molecules or atoms of gas colliding with the surface of the object (Fig 2. 1.1). Each gas atom acts as an individual 'hot forge'. For examples, at 900°C and 2MPa (typical of the welding parameters of titanium alloys) the gas atoms move at a velocity of around $800ms^{-1}$ and approximately 10^{28} collision events occur per square meter per second. These tiny atomic forges have the ability to reach all surfaces of the component, including re-entrant angles, and to act reliably and consistently independent of shape. On average, the numbers of gas atoms moving through unit area, and their velocities, are the same in all directions. Thus, the pressure on every surface of a component being processed is the same and acts in a direction normal to the surface (Fig 2.1.2).

2:1:2 Advantages of HIPing

The major reasons for using hot isostatic pressing as opposed to unidirectional pressing are as follows[5]:-

a) No rams or dies are being used in HIP, therefore, no wall friction are developed or no lubricant are required.

b) A coherent metallurgical weld can be achieved across a large interfacial area with many re-entrant angles by the HIP diffusion welding process, whereas in conventional diffusion welding, the uniaxial pressure restricts the joint geometry to a butt arrangement.

c) In the conventional diffusion welding deformation may start to occur near the surface before the removal of the pores, which might lead to distortion. But in HIPing, microplastic deformation is concentrated only in the contact area, without causing any bulk distortion.

d) In unidirectional welding, complex cylindrical weld is extremely difficult to process. On the other hand, through the HIP route it could be easily achieved.(Fig-2.1.3 a)

e) Ceramics-metals welding can be achieved by the help of isostatic pressure which causes flow of metal to the surface defects and the undulations on the surface of the ceramics. This flow generates a mechanical interlocking.(Fig: 2.1.3 b) even where interdiffusion is limited.

f) With HIP diffusion welding, powders and porous bodies can be simultaneously densified and welded to a substrate. This is not possible with conventional diffusion welding.

g) Components with larger dimensions require larger uniaxial presses as the load increases with increasing welding area whereas no area dependence exists for parts to be HIP welded. The only limitation is the size of the HIP-unit.

2:1:3 HIPing Mechanism

A large number of papers describing the mechanism of HIP process as well as respective models have been published in the last 3 decades[6-11]. The best comprehensive analytical study of the mechanism of deformation and densification during HIP was made by Arzt, Ashby and Esterling[11]. This analytical work elegantly defined the various mechanisms during densification in term of deformation mechanism maps and provided the first basis for a scientific understanding of HIP mechanism. These work defined five mechanisms of HIPing: plastic yielding, power-law creep, diffusional densification, enhanced diffusional densification when the grain size is much smaller than the particle or the void size, and the separation of pores from boundaries when grain growth occurs.

Several mechanisms contribute to densification or removal of interfacial voids during hot isostatic pressing. When a pressure is applied, it is transmitted as a set of forces acting across the interfacial or particle contacts. The deformation at these contacts is at first elastic, but as the pressure rises, the contact forces increase, causing plastic yielding and expansion of the points of contact into contact areas. Once these contact areas can support the forces without yielding, time dependent deformation processes such as power law creep and/or superplasticity in the contact zones, and grain boundary and lattice diffusion to the void surface start to occur. During HIPing the specimen is usually held for a considerable time (half an hour or more) at a high temperature (0.5-0.7 T_m, where T_m is the melting temperature). This can result in grain growth, to minimise grain boundary energy, and pore isolation from the grain boundaries. When the pores no longer lie on grain boundaries, densification by diffusive mechanisms is suppressed. Second phase particles and impurities can help to pin grain boundaries and pores themselves may also pin boundaries before being separated. Power law creep and plastic flow are not, of course, affected by pore separation[11].

2:1:4 The HIP unit

The HIPing process for diffusion welding relies on heating of a gas to a temperature typically in the region of 500-1200°C and a pressure of 2-25 MPa. The energy stored at the temperature and pressure is large, placing high demands on high quality design of pressure vessel and workmanship to ensure operational safety. The principal requirements for the pressure vessel material are tensile strength, fracture toughness and fatigue strength. Fracture toughness is perhaps the most important of these because the large quantity of elastic strain energy may be stored in the material under pressure[5]. The probability of fast catastrophic fracture occurring in the vessel must be negligibly small. It is always necessary to test non-destructively the vessel at regular intervals during its life time to check for the development of cracks, for this reason the vessel should be designed to allow easy inspection. The end closures are potential points of weakness and their design is critical. There are two main styles - one is the external yoke closure and other

one is the resilient threaded-end closure. To improve operational safety further, it is advantageous to construct an energy absorption protection shield around pressure vessel.

Considering the relative position of the furnace heater and pressure vessel, there are two kinds of vessel which are as follows:

i) *Hot wall vessel*: where the furnace heater is placed outside the pressure vessel, is limited in pressure and temperature capability by the creep strength of the vessel materials.

ii) *Cold wall autoclave*: where the heater is placed inside the pressure vessel, requires large pressure vessels but meets high pressure and temperature requirements with fast loading and unloading of the charge.

Care should be taken in designing HIP furnace. Another important point to be noted here that the pressure is being developed by argon gas which could lower the oxygen level in the surrounding in case of leaking. Sufficient ventilation should be made around the HIP furnace.

2.1.5 Application of HIP

The HIPing process was initially developed as a means of diffusion welding of nuclear reactor components and for the removal of porosity in hard materials. However, the major commercial activity now centers upon the consolidation of powder materials and on the densification of high-performance castings. The common HIPing application in a generic way, are the following:[5]

a) *Diffusion welding:* Diffusion welding of similar and dissimilar materials is performed by HIPing which can overcome the problems of conventional joining and uniaxial diffusion welding techniques.

b) *Upgrading of casting:* Densification and weld-up of cracks of the castings can be done by removing macro and microporosity as well as flaws of aluminium, copper and titanium alloys, steels and also nickel and cobalt based superalloys.

c) *Densifying pre-sintered components:* Theoretical density of WC hard metals, Si_3N_4 and other advanced ceramics can be achieved with avoiding excessive grain growth.

d) *Shaping and compaction of encapsulated powders:* Tool steel, nickel and cobalt based superalloys and also ceramics and metal matrix composites (MMCs) are produced by HIPing of their powders in a gas-tight envelop.

Now-a-days superplastic forming of complex shape with concurrent diffusion welding is also an exploring field of HIP. Hence, in spite of the other applications of HIP, HIP-diffusion welding is the unique process for the welding of complicated shapes.

2.2 DIFFUSION WELDING

2.2.1 Introduction

Several welding methods have been developed to date, and from a metallurgical point of view these may be classified into two categories: a) Fusion Welding process and b) Solid-State welding process. In fusion welding the two edges or the surfaces to be joined are heated to the melting point and where necessary, molten filler is added to fill the joint gap. Such weld comprises three distinct zones: the fusion zone, the unmelted heat-affected zone (HAZ) adjacent to the fusion zone, and the unaffected parent metal (Fig-2.2.1a). Solid-state welding, on the other hand, are made by bringing two clean solid surfaces into atomic contact for a metallic bond to be formed between them (Fig 2.2.1b).[12] Solid-state welding is generally further classified into two groups: diffusion welding without a large amount of plastic deformation and welding accompanied by extensive plastic deformation, as in roll welding, friction welding, cold pressure welding, explosive welding, ultrasonic welding etc.

Among the above processes, diffnsion welding has been increasingly used in aerospace, nuclear, and other applications. In this technique two clean metallic snrfaces are brought into contact at elevated temperatnre under a moderate pressure. If two perfectly clean, atomically flat surfaces are brought into intimate contact, the interatomic forces become active to form strong metallic bonds at the equivalent of a grain boundary and thus a perfect join will be created without the need for heat and pressure. Diffusion welding is merely the practical extension of this approach to real surfaces which are neither atomically flat nor perfectly clean, temperature and pressnre are applied to the work-pieces to ensure good metal-to-metal contact and joining at the interface[3, 13].

2.2.2 Advantages of diffusion welding

The major reasons for using diffusion welding as opposed to other welding or adhesive bonding are as follows:-

1. Since no melting or additional materials are involved, there is no discontinuity in the microstructure and therefore uniform properties can be achieved at the weld region similar to parent metals.

2. The pressure required for welding is very low with respect to the yield strength of the material, there is virtually no distortion of the components during welding, nor any temperature gradients developed which may lead to distortion during and/or following welding. Diffusion welding is therefore a net shape forming process.

3. For the sheet materials, large area can be welded along with superplastic forming to produce complex honeycomb structures.

4. Those materials which can not be welded by fusion welding but have ability to dissolve the surface contaminants (i.e. titanium alloys), have been successfully welded by diffusion welding.

2.2.3 The mechanism of diffusion welding

When pressure, P, is applied to a DW couple, the points of contact between the two surfaces will first deform by plastic yielding. This causes the average contact area, f_c, to grow and the effective pressure to fall until the yield stress, σ_{ys}, of the material is no longer exceeded(Fig 2.2.2). At this stage the weld zone consists of an `island' of contact (bond) randomly distributed in a `sea' of empty space. The `sea' of space may be considered as a planner array of very irregularly shaped voids. The aspects ratio of the voids is governed by the roughness profile of the original surfaces. The major time of the diffusion welding process is spent in void closure. The elimination of the interfacial voids can occur by three distinct processes:[1]

(a) plastic collapse of the planner array of very irregularly shaped voids by time-dependent power law creep and / or superplastic flow.

(b) stress directed atomic diffusion into the voids via both grain boundary and bulk of the materials.

(c) mass transfer from one region of the voids to another by surface diffusion or vapor phase transport.

Only the first two mechanisms (a) and (b) actually reduce the volume of the interfacial voids. Plastic collapse results the lateral expansion of supporting materials and also transport the materials into the voids due to the applied stress (Fig-2.2.3a). The voids closure mechanisms in the last category (c) are driven by differences in the chemical potential arising from variations in the surface curvature of the individual voids. Redistribution of material around the surface of the interfacial voids does not give rise to any reduction in void volume. However, the change in void shape alters the cross-sectional area of the voids in the weld interface and thus has an apparent or secondary effect on the kinetics of welding.(Fig-2.2.3) [1].

Driving Force for Void Closure During diffusion welding

An atom in the surface has a relatively high energy compared with an atom in the bulk. This occurs because the atoms in the free surface have no neighbours on one side and hence one third of its nearest neighbours is missing. Grain boundaries and dislocations are also regions of disorder and therefore they are also zones of high energy relative to the perfect crystal in the bulk. But the specific surface energy of interfacial voids or pores is greater than the grain boundary energy. Therefore from a thermodynamic standpoint, voids should be eliminated first from the system. The driving force (DF) for the void closure during HIPing are the surface energy and the effective stress (σ_{eff}) developed due to the applied external pressure.

$$D.F = \frac{2\gamma}{r} + \sigma_{eff}$$

Diffusion occurs both through the lattice and along grain boundaries in response to the stress. The void thus collapses through diffusion and creep processes. The movement of an atom from its original position in the crystal lattice into a vacancy, or into an interstitial position, requires thermal (activation) energy. Different diffusion routes have different activation energies(Q). The plots for diffusion via the surface, the grain boundary and the lattice are shown in Figure 2.2.4 where D is the diffusion coefficient and T is the absolute temperature. Activation energies tend to be in the region of a few electron-volts in magnitude. Among these three routes for diffusion, surfaces are the regions of relatively high disorder therefore the activation energy for diffusion is also low. Whereas activation energy for the lattice is the highest and that of the grain boundary is in between. Thus, the lattice line in the Figure 2.2.4 has the highest slope and the surface line the lowest. As a result, at lower temperatures (higher 1/T) grain boundary and then surface diffusion dominates. The change from one predominating mechanism to another depends on the cross-sectional area of the short-circuit paths (i.e. grain boundaries and surfaces) available. If a material has a fine grain size, the cross-sectional area of short-circuit paths will be much higher and lattice diffusion will only be prevalent at relatively high temperatures. For such a situation to exist, the grain size G must be small. The effect of decreasing grain size is shown schematically in Figure 2.2.5. Smaller grain size is also an essential requirement to show superplasticity which would help in HIP diffusion welding of superplastic materials.

2.2.4 Factors affecting Diffusion Welding

The extent of welding and the way in which it is achieved has been considered to be controlled by three groups of factors.

(a) Process parameters: the four principle variables are surface preparation (surface roughness), time, temperature and pressure.

(b) Material Properties: such as grain size, crystal structure, diffusivity, microstructure, oxide stability (chemical activity) and mechanical properties.

(c) Metallurgical factors: such as the formation of intermatallic phases during welding and mutual solubility of dissimilar metals.

Most of the mechanisms operating in diffusion welding are controlled by these factors, which may themselves be related to each other[24].

2.2.5 Modeling of Diffusion Welding

Several models have been developed to predict time, temperature and pressure needed to remove interfacial voids i.e. for the complete interfacial contact between two surfaces of varying roughness[2,4,15-19]. Along with the optimization of the process parameters, the models of DW also provide better understanding of the mechanisms involved during welding. Almost all the models simplify the geometries of the contacting surfaces and presume that they can be treated as a series of identical asperities touching at their tips to create an array of identical voids. The way by which a typical void is removed is then studied in the various models.

The first attempt to predict the time required to form a sound weld between two rough surfaces was made by Hamilton[4]. The model assumed that the surfaces to be joined consisted of triangular section asperities in point-to-point contact (Fig 2.2.6). The asperities were thought to collapse by time-dependent plasticity under plane strain conditions. The average stress, σ, in the triangular section asperity was related to the applied pressure ($\sigma = \sqrt{3}$ P). The welding time, t_w, was then calculated by dividing the displacement required to fully collapse the asperites by the average axial strain rate. This simple model was later extended by Garmong et al[15] to describe a more realistic surface geometry. In the later model the surfaces to be welded were considered to consist of short wavelength asperities superimposed on a longer wavelength roughness (Fig 2.2.7). The diffusion welding process was divided into two-stages. In the first stage, long-wave length surface asperities were assumed to be flatten by time dependent plastic collapse and the time taken for the interfacial channels to reach the dimensions of the short wavelength roughness was calculated numerically. In the second stage of welding process, interfacial

diffusion was believed to be the dominant void closure mechanism and the time taken to sinter the planar array of spherical voids created by the short wavelength roughness (Fig 2.2.8) was calculated . The total welding time was taken to be the sum of the two seqnential processes.

A further refinement of the plane strain models of diffusion welding was introduced by Derbey and Wallach[6], who considered diffusion welding to be analogous to pressure sintering[7]. The following bonding mechanisms were postulated:

1) surface diffusion from surface sources to a neck
2) volume diffnsion from surface sources to a neck
3) diffusion along the bond interface from interfacial sonrces to a neck
4) volume diffusion from interfacial sources to a neck
5) power law creep
6) plastic yielding deforming the ridge.

The six mechanisms have been described in three groups illnstrated in Figure 2.2.9, each of which have common sonrces and sinks of mass transfer. In this model initial surface contact was considered as involving a series of long triangular ridges contacting peak to peak (Fig 2.2.10). Welding was assumed to occnr in three stages, each with individual geometry. Stage 0 is instantaneous plastic flow until sufficient contact area is achieved, a diffusion-dominant (time-dependent) stage 1 based on straight-sided void geometry until the void aspect ratio reached unity and a stage 2 in which removal of circnlar cross-section void geometry took place (Fig 2.2.11). Rate equations for each of the seven mechanisms operating independently in stage 1 and 2 are summed to give an overall void shrinkage rate and a total welding time.

The above models assume that welding occnrs under plane strain condition (in unidirectional welding), whereas in HIP diffusion welding the condition shonld be isostatic compressive stress state. Although the same physical mechanisms of void closure are operative, the kinetics of each process will differ from those under plane strain

conditions and will lead to a reduction in welding time. However, there is some controversiallity in approximating the interfacial voids and hence measuring the stress distribution around the voids. A mathematical model describing the filling of cylindrical voids under isostatic pressure was developed by Pilling and later on refined by Islam predicted the DW time claiming more satisfactory results compared with the experimental DW time[2]. There have still tremendous dimension to upgrade these models considering other factors.

2.2.6 Testing of Diffusion Welding

At first, metallography could reveal the idea about the sound weld by sectioning at several portion of the welded specimens. Light microscopical analysis is generally carried out to observe the microstructure of the welded samples. The samples are cut perpendicular to the weld interface and standard metallographic technique is used to polish. The unetched structures may also reveal the voids at the weld line. The number and size of the voids are indicative of the weld strength. Actually in case of etched microstructure of the sound weld, the weld line should be indistinguishable and there should be no weld zone found in similar materials. For the metallographic examination, a sound weld is one which shows no evidence of the voids throughout the weld line in the sample[2].

The quality of diffusion welds can only be reliably assessed by comparing the shear strength of the weld lines with those of parent metal after a simulated welding heat-treatment cycle to it. A number of mechanical tests have been devised to assess the quality of diffusion welds. In the case of welds produced in thick sections, conventional tensile and impact test pieces can be readily produced and the fracture strengths can be compared with that of the parent metal. In practice, parent metal tensile strengths are often achieved in welds with more than 85% interfacial bonding, while parent metal fatigue endurance normally requires a complete absence of interfacial micron voids[3].

Impact testing is not widely applicable because the majority of diffusion weld are formed between sheet materials. In such cases, the fracture strength of the join is measured using

a constrained lap shear test although no test piece standard exists[3]. The typical non-destructive testing widely used in fusion welding is nearly inapplicable to diffusion welding because of the small size of the defects that usually occur (defects each with a surface area of higher than $0.5mm^2$ and higher than $1\mu m$ wide may be detected by ultrasonic testing). The liquid penetration, eddy-current and magnetic-particle methods of non-destructive testing may be used to some extent to detect external and subsurface flaws in the testing of diffusion welded products.

2.2.7 Superplasticity and Diffusion Welding

The discussion of superplasticity along with Diffusion welding is obvious. The reasons are two folds: first is that the process of diffusion welding is accelerated by superplastic flow[13] and the second is that diffusion welding is now widely used in combination with the superplastic forming[3].

The term superplasticity is used to describe a material's property which shows high strains without the formation of unstable tensile necks. For deformation in uniaxial tension, elongations in excess of ~300% are indicative of superplasticity, while values of >1000% are not uncommon. The highest elongations recorded in the literature are 4850% for a Pb–Sn eutectic[20], and 5500% for a complex commercial aluminium bronze[21], althongh Higachi has recently reported an elongation of >8000% for the latter material[22] These materials, however, show no microstructural evidence of deformation. The grains remain equiaxed and careful experimentation has shown that no recrystallization takes place. Indeed, the grain remain undeformed despite large imposed strains. The deformation takes place by the grains moving with respect to one another and is generally considered to be controlled by grain boundary sliding and grain rotation[34]. Sliding between two grains must involve accommodation at the intersection with a third grain and may involve diffusion and/or dislocation processes. Diffusional processes can involve both bulk diffusion and grain boundary diffusion.. To show snperplastic behavior a material must have the following four requirements:

1. The temperature must be above $0.5T_m$ so that diffusion controlled deformation mechanisms predominate.

2. Strain rates must be neither too high nor too low (about 10^{-3} s^{-1}) so that diffusive deformation mechanisms start to dominate over dislocation mechanisms.

3. The grain must be equiaxed to allow easy grain switching and small (typically < 10 μm) to reduce diffusional distances.

4. The grain must not grow during processing.

If the above conditions are fulfilled and maintained, then a material will show a high strain rate sensitivity (m) of flow stress over a strain rate range of 10^{-5} - 10^{-1} s^{-1}. The m value is defined by the relationship.

$$\sigma = K\dot{\varepsilon}^m$$

where σ = steady state flow stress, $\dot{\varepsilon}$ = imposed strain rate, K = material constant. Although a fine grain size is an important requirement for superplasticity, it is not the only parameter to characterise the superplastic microstructure. The grain boundaries between adjacent matrix grains should be high angle disordered because grain boundary sliding (GBS) is the predominant mode of deformation during superplastic flow. Other factors such as grain aspect ratio, grain size distribution, texture, and the volume fraction of phases and their deformation characteristics, can also influence superplastic behaviour[23,24].

Superplasticity may be observed in single phase materials, but it is much more commonly associated with two-phase alloys, which are considerably more resistant to grain growth. Intergranular second-phase particles, which pin grain boundaries, provide such an impediment, but grain growth even more restricted in "micro-duplex" equiaxed alloys. These are two-phase materials having fine grained microstructure with approximately equal volume fractions of the phases, and for which grain growth is restricted markedly as a

result of frequent interphase grain contacts of the chemically and structurally different phases. Procedures for grain refinement in duplex alloys, have been described by Wert[25] and by Pilling and Ridley[3] which often involve the hot working in the two phase field close to the superplastic temperature range. Such thermomechanical processing will be described in the next chapters with specials reference of titanium alloys.

(a) The role of superplasticity in Diffusion Welding

Following the discovery of the superplastic phenomenon, it was pointed out in early studies that the properties of superplastic materials have a potential utility in the solid state welding area. The early review article on superplasticity by Underwood[26] to suggest that the high ductility of superplastic materials may be used to accelerate the joining process between contacting interface in the solid state welding.

The diffusion welding efficiency is the highest at temperatures in the region of maximum superplasticity. Superplasticity contributes at least to the initial stages of the welding process. Flow stresses involved in diffusion welding may lead to microplastic deformation in the vicinity of the welding interface and at asperities and, in some cases, this deformation may be useful in breaking a surface oxide film.

(b) Superplastic forming(SPF) with concurrent Diffusion Welding

Superplastic deformation is characterized by high strain rate sensitivity (m) of flow stress over a strain rate range of 10^{-5} - 10^{-1} s^{-1}, and this, combined with a high resistance to non-uniform thinning, has led to the SPF of near net shapes from sheet materials using techniques similar to those developed for the bulge forming of thermoplastic (Fig-2.2.12a). The combined application of superplastic forming and diffusion welding(SPF-DW) to produce a component in one heat leads to an almost unlimited design flexibility, the cost saving in comparison to other fabrication methods reaches value up to 60%. This value has been substantiated by a wide range of design-to-cost studies conducted by aerospace companies through out the western world[27-29]. The basic techniques of SPF-

DW are illustrated schematically in Figure-2.2.12 b and c for the production of an integrally stiffened and honeycomb structure and a sandwich structure, respectively.

2.2.8 Diffusion Welding of Superplastic titanium alloys

The diffusion welding technique has been widely adopted in the joining of titanium alloys, because of their very poor fusion weldability. The ease with which titanium can be welded may be attributed to the ability of titanium lattice to take into solution both its surface oxide and other contaminants when subjected to a moderate pressure at elevated temperatures[3] Among the titanium alloys, there are many examples using the superpalsticity of α/β duplex phase alloys, such as Ti-6Al-4V, Ti-6Al-2Sn-4Zr-2Mo and Ti-4Al-4Mo-2Sn-0.5Si (IMI550) which are readily welded at temperatures from 880^{O}C to 940^{O}C with applied pressures between 0.6 to 3 MPa for process time up to 2 hours[3,17]. These duplex phase alloys when prepared with a very fine grain structure, are known to exhibit extensive superplasticity within the temperature range 750^{O}C to 950^{O}C, when the microstructure is preserved with equiaxed α-grains within the β-matrix. So, diffusion welding temperature of these alloys is often selected to be within the temperature region giving optimum superplasticity. The relative ease with which solid state diffusion welds can be formed in titanium alloys is reflected in the growing body of literature and its acceptance as a mainstream manufacturing technology[25,26,30].

2:3 TITANIUM ALLOYS

2:3:1 Introduction

The research on Titanium (Ti) alloys had explored violently after the 2nd world war. The relatively low density and high melting point (1678^{O}C) of titanium made it attractive as a potential replacement for aluminum for the skin and structure of high-speed aircraft subjected to aerodynamic heating[31]. The specific strength of titanium alloys when compared with other light alloys, steels, and nickel alloys is apparent in Figure 2.3.1[31]. So, in its specific strength up to 500^{O}C titanium has no competitors among industrial alloys. This advantage has led to the universal acceptance of titanium in the aerospace industry - often to manufacture many aircraft's units and parts from the engine to bolts and nuts. Titanium tanks are excellent for storing liquid oxygen and hydrogen: at super low temperature it does not disintegrate like most other metals, but, on the contrary, gains in strength. Hence, space-age technology will not be able to do without titanium either. Around 80% of the total production of titanium is used in this way. Most of the remainder is used in the chemical industry due to its outstanding corrosion resistance property[31-34] Titanium alloys show a wide range of mechanical properties as a result of both modification of alloy chemistry and thermomechanical treatment. For this reason more than twenty different titanium alloys are employed in aerospace applications alone, and novel processing routes still appear regularly in patent applications[35].

2:3:2 Classification and Phase diagrams of titanium alloys

Titanium is an allotropic metal as like as iron. It has a closed-packed hexagonal(hcp) structure (a= 2.953 Å and c= 4.729Å), called alpha(α) at room temperature. This alpha transforms to body-centered cubic beta(β, a=3.327Å) phase at 883^{O}C which remain stable up to the melting point. The addition of alloying elements to titanium will influence the α

to β transformation temperature. It is common practice to refer to alloying elements as α or β stabilizers.

An α stabilizer means that as solute is added, it dissolves preferentially in the α phase, and hence it expands this field with raising the α/β transus temperature. Similarly beta stabilizer depress the α/β transus and stabilize the β–phase field[31-33]. Alloying elements with the electron/atom ratios of less than 4 stabilize the α–phase, elements with a ratio of 4 are neutral and elements with ratios greater than 4 are β–stabilizing. Except hydrogen, other interstitial elements oxygen, nitrogen, and carbon raise the α/β transus. Al, V, Si, have the bonding electrons 3,5,4 respectively and hence Al is a α–stabilizer, V is a β–stabilizer and Si is neutral in its effect on either phase. Zirconium, Tin are also neutral which are added to the Ti-alloys for solid solution strengthening.

In commercial applications binary alloys are rarely used. The properties of them can generally be improved by the carefully engineered addition of further alloying components. Thus, for examples commencing with Ti-Al, the addition of Sn has led to the technical α–alloy Ti-5Al-2.5Sn and the addition of V to the popular Ti-6Al-4V. Substitutions of Ta for Nb and/or Zr for titanium have improved the superconductive properties of Ti-50 Nb and resulted in technically important ternary and quaternary superconducting alloys. In structural alloys, the additions are chosen to achieve improvements in mechanical properties such as strength and toughness, structural phase and chemical stability[34]. The relative amounts of α and β stabilizers in an alloy (and heat- treatment) determine whether its microstructure is predominantly one-phase α, mixture of α and β or the single phase β (or non-equilibrium product of β) over its useful temperature range[33].

<u>α–alloys :-</u>

Commercially pure titanium and Ti-5 Al-2.5 Sn are the commonly used α–alloys, having single phase, high thermal stability leads to reasonable creep strength at the upper temperature range. Although they have low tensile strengths at room temperature, display good ductility aud strength down to very low temperature and this is why they have been

used in cryogenic storage tanks. As it is usually necessary to hot work the alloy at temperatures below α/β transus in order to prevent excessive grain growth, formability is limited because of their hexagonal crystal structure and the fact that they exhibit high rate of strain hardening[31].

α+β alloys :-

These contain sufficient solute elements to produce a broad α+β phase field extending down to room temperature. A much wider range of microstructures can be produced in such alloys than is possible in α alloys. In α alloys such as Ti-Al system, the two phase α+β region is narrow and exists at higher temperature (in Fig-2.3.2a). Figure -2.3.3a, shows temperature versus V concentration curve for two fixed levels of Al, whereas Figure -2.3.3b, shows a complementary function in terms of a continuous variation of the Al concentration at four levels of V. From these two figures it is clear that the introduction of V at constant Al concentration, produces a rapid decrease in the (α+β) to α boundary, although it has a comparatively small influence on the position of the β transus.

The alloy Ti-6Al-4V could be regarded as being derived from unalloyed Ti by (1) the addition of Al to produce solution strengthening and raise the β transus, and (2) the addition of V to lower the (α+β) to α boundary[34]. The result is that the α+β phase field is increased as such that the β transus temperature is about 980°C and (α+β) phase field exists even at room temperature.

β–alloys :-

The β alloys are characterized by sufficient β stabilizers to ensure the retention of the bcc β phase on rapid cooling to room temperature. Strengthening by α–phase particles is then achieved during heat treatment[34]. Alloys of this type attracted early attention because of the superior forming characteristics anticipated for the bcc structure.

2:3:3 Effect of Heat treatment on microstructure and properties

The allotropic transformation of titanium during cooling from β to α offers, by analogy with steel, the prospect of various microstructures through different cooling rates. Heat treatment of Ti alloy may be conceivable by bearing in mind that nucleation of the cph α-phase from the bcc β– phase is difficult if no intermittent equilibrating is done in the α+β phase fields. This is why unalloyed titanium also undergo martensitic transformation and even very slow cooling from β–phase will not yield equiaxed α–grain. If the alloy has been given time i.e. solutionized in the α+β phase fields, equiaxed α-grains will form, whereas it is not necessary to hold carbon steel in the α+γ field for getting proeutectoid equiaxed ferrite. We know in a coarse austenitic structure at high temperature, difficulty of nucleation (due to smaller number of triple points of grains and moderate cooling rate) suppress the formation of massive ferrite, and Widmanstätten structures are developed. So, it is obvious for the titanium alloys (as transformation from bcc to hcp is sluggish) to get the Widmanstätten morphology at the slowest practical cooling rate. Furnace cooling produces coarser Widmanstätten α–plates than air cooling. β–stabilizer rich β–phase remains as a thin layer between the Widmanstätten Al- rich α–plates[31,34,36](Fig 2.3.4).

In contrast to above nucleation- and- growth types of phase change which rely on thermally activated atomic diffusion, the second important transformation of titanium alloys is the formation of martensite that take place when β is cooled rapidly by water quenching, involve a cooperative movement of atoms resulting in a microscopically homogeneous transformation of one crystal lattice into another. The ideal martensitic process itself is not thermally activated and takes place at high temperature-independent speeds ; but in practice a clear-cut separation of transformation process into "nucleation-and-growth" and martensitic is generally not possible. Although in pure metals such as unalloyed titanium, a simple athermal martensitic transformation conceivable, in an alloy the situation is more complicated. The alloying inhibit the movement of atomic planes and thereby reduce the speed of the transformation, thus bringing it into competition with the

nucleation-and-growth mechanism. Unalloyed titanium transforms martensitically during cooling through its $\beta \rightarrow \alpha$ allotropic transformation temperature, 883°C.

In alloys of Ti, the $\beta \rightarrow \alpha^m$ transformation temperature, M_s is composition dependent. In α–stabilized alloys, typified by Ti-Al, M_s may lie a little below the $(\alpha+\beta)$ to α boundary; whereas in the β–stabilized alloys it always lie within the $\alpha+\beta$ field[34]. Figure- 2.3.5 shows a typical binary β-isomorphous system with a schematic diagram which depicts trends in tensile strength with respect to alloy content resulting from different heat treatments procedures.

It will be seen that the strength of annealed alloys increases gradually and linearly as alloy content, or percentage of β-phase, increases. Rapid cooling results martensitic structure and/or retained β and after aging different microstructures could be achieved - hence a more complex relationship exits between the strength and composition. Here, the martensite of Ti-alloys is not as hard as ferrous martensite. Again due to obvious reason the retained or metastable β is soft. So, very soft structure might be found where 100% metastable β (where M_s temperature occurs at room temperature) are available by quenching. On the other hand these compositions provide the maximum response to strengthening if the quenched alloys are aged to decompose the retained β.

M_f for β containing Ti-6Al-4V is above room temperature so that quenching from above the β transus temperature produces a fully martensitic structure (Fig 2.3.6a). The martensite can be aged by heating to temperatures where appreciable diffusion can occur, in which case the supersaturated α' can decompose by the precipitation of β on the martensite plate boundaries and dislocations. (Fig 2.3.6b)

Alloys for engineering applications are not usually used as with the above condition which can be found from β–phase field, but are hot-worked in the $\alpha+\beta$ region of the phase-diagram in order to break up the structure and form equiaxed α–grains. This is usually followed by annealing at 700°C which produces a structure of mainly α with finely distributed retained β (Fig 2.3.7) The advantages of this structure is that it is more ductile

than when the α is present in a Widmanstätten form. If the alloys is held lower in the α+β field before quenching the β–phase that forms can be so rich in β–stabilizer (here V) that the M_s temperature is depressed to below room temperature and quenching results in retained β[36].

Some mechanical properties also differ for such phase-region dependent forming processes. The most important properties deteriorated by the change in structure resulting from processing in the β field rather than α+β regime, is ductility[35,37]. This reflects the substantial enlargement of the microstructural unit size resulting from the rapid grain growth in the β field. For titanium alloys, fracture toughness may be increased by β processing to give microstructures containing an α platelet morphology[38-41]. But, the fatigue crack growth rate is lowest for Widmanstätten structures resulting from β processing, and the highest for an equiaxed α morphology[43]. This is attributed to the much more tortuous crack paths across α plates and along α/β interfaces in the Widmanstätten structure and with the higher incidence of multiple cracking as compared with α+β processed material.(Fig-2.3.8)

Again the presence of β phase renders the creep resistance inadequate for higher temperature applications. To achieve a good balance of creep and fatigue properties in α/β alloys, a duplex structure consisting of about 30 volume % of equiaxed-α combined with Widmanstätten-α is favored for rotating component, such as compressor discs, that operate at high temperatures.

2:3:4 High temperature deformation of Titanium alloys

Having reviewed the alloy types, and their microstructures and associated mechanical properties in relation to processing conditions, it is pertinent to discuss some general characteristics of the deformation process itself and some recent improvement in the forging and microstructural development of titanium alloys.

The most important distinction to be made between the α and β phases is that diffusion is much faster in β at any given temperature. In pure titanium, at the allotropic transition from α to β at 883°C the diffusivity increases by nearly three orders of magnitude[35], and in alloys diffusion is a hundred or more times as fast in β as in α. Consequently, processes of diffusional deformation and of recovery and recrystallization occur at lower temperatures and high strain rates in β phase than in α. At temperatures at which β becomes the continuous phase, the flow stress reflects the character of this phase rather than the isolated α particles which then behave like hard inclusions in the soft β matrix. Figure 2.3.9 shows this phenomenon for commercial β, α+β, and near α alloys which reflects this point[35].

The practical limits of working temperature are set by excessive grain growth and surface contamination by absorption of oxygen and nitrogen at high temperatures, and by excessive deformation loads and the onset of shear banding at low working temperature[44].

Again, in order to select the forging temperature it is necessary to know the β transus and the temperature at which a specified amount of primary α remains. Figure 2.3.10 shows the temperature of the transus and the width of the α+β field for a wide range of titanium alloys. From this it can be seen that α+β working region of α and near-α alloys is limited to a very narrow temperature regime, as small as 30°C in some cases, and that in β alloys the α+β working regime is restricted by the very low temperatures involved. It is important to obtain as wide a processing window as possible and to know how α fraction varies with temperature. To this end, β approach curves have been determined for a range of titanium alloys; some examples are shown in Figure 2.3.11. Ideally the α+β field should be as wide as possible within the practical range of their fabrication temperature[35].

FIGURES

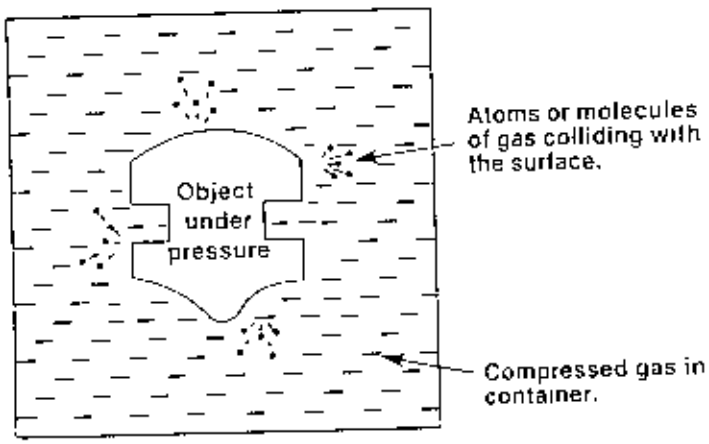

Figure 2.1.1 Pressure arises from atoms or molecules of gas colliding with the surface of the object being hot isostatically pressed (HIPped).

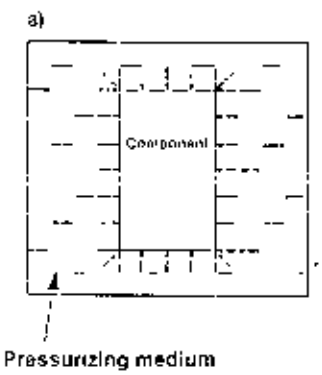

Figure 2.1.2 In isostatic pressing the forces on the component are the same in all directions.

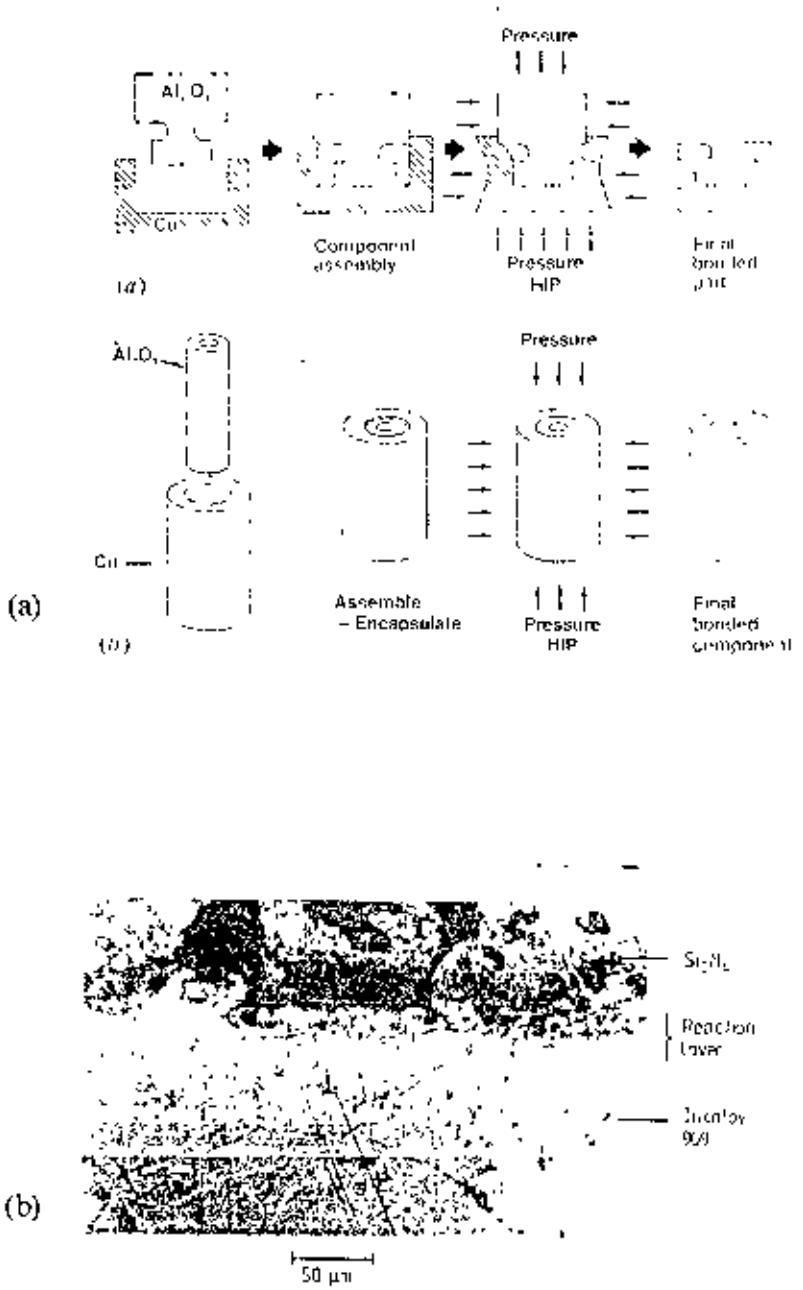

Figure 2.1.3 (a) Schematic diagrams of cylindrical welding processes by HIPping. (b) Micrograph of weld between Incoloy 909 to silicon nitride (Metal-Ceramics welding). The metal has flowed into the undulation of the ceramic surface. A reaction layer is also viewed

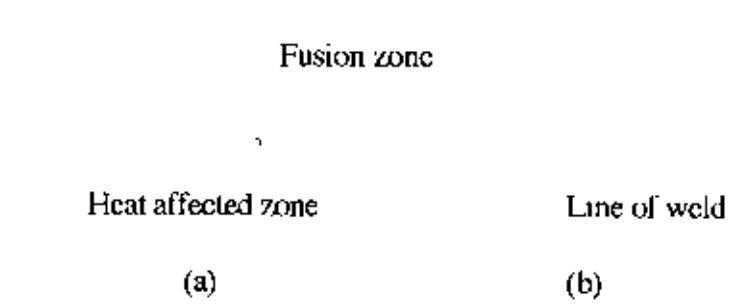

Figure 2.2.1 Schematic diagrams of (a) Fusion Weld and (b) Solid Phase Weld.

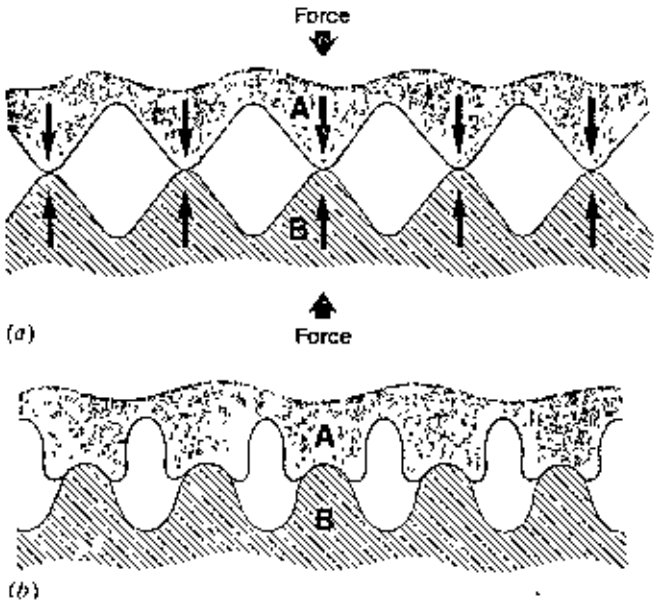

Figure 2.2.2 (a) Magnified view of a region where two materials come into contact showing surface roughness. (b) Magnified view of the same region after microplastic deformation.

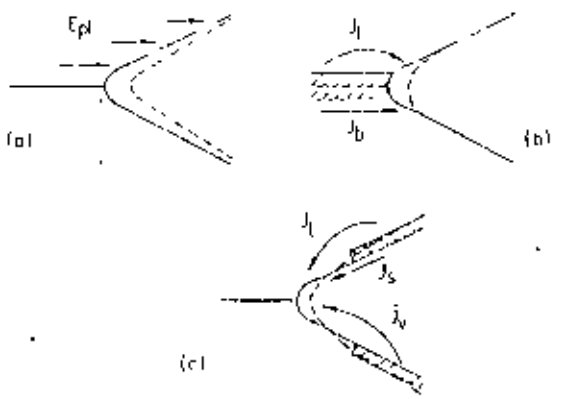

Figure 2.2.3 Schematic illustration of mass transfer paths for diffusion welding. (a) Time-dependent plastic flow (b) diffusion from interface to cavity via the lattice and the boundary and (c) diffusion from around the surface of the void via the lattice and via the vapor phase

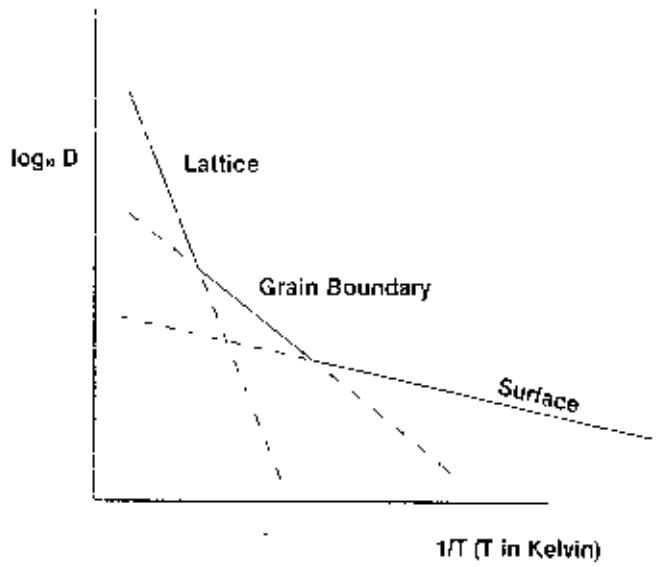

Figure 2.2.4 Plots to show the temperature dependence on the surface, grain boundary and lattice diffusion.

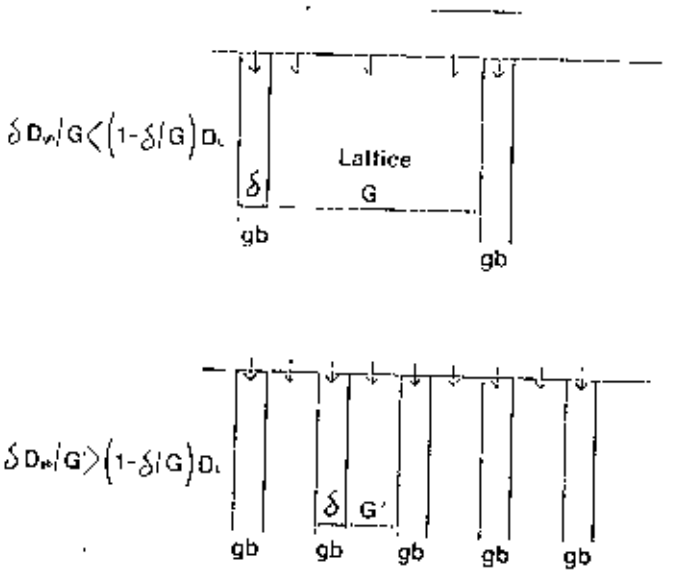

Figure 2.2.5 The effect of decreasing grain size to increase the predominance of grain boundary (gb) diffusion over that arising in the lattice.

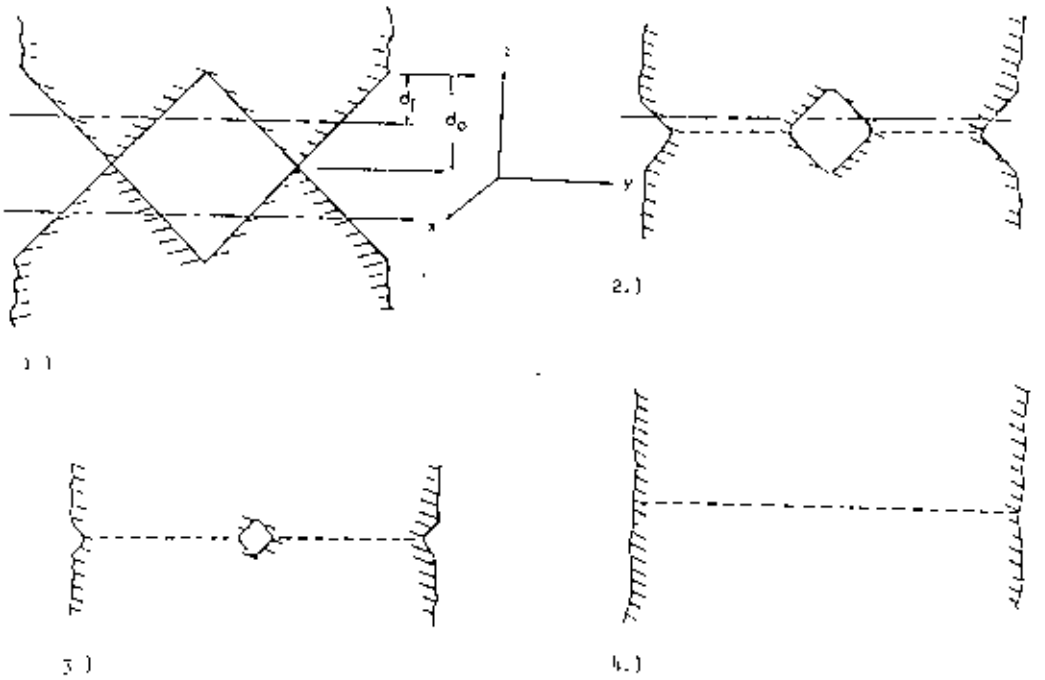

Figure 2.2.6 Hamilton's triangular surface asperities meeting point-to-point across the weld interface and the sequence of deformation.

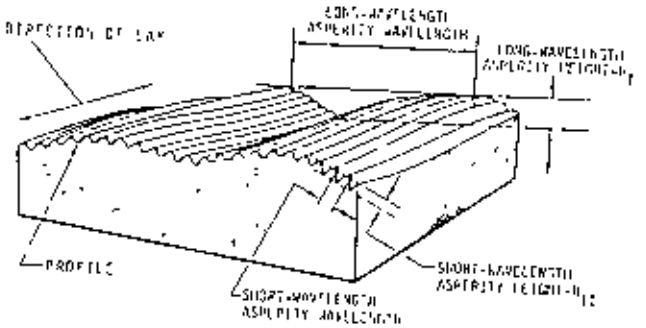

Figure 2.2.7 Sketch of the surface asperities and terminology used in the Garmong et al model.

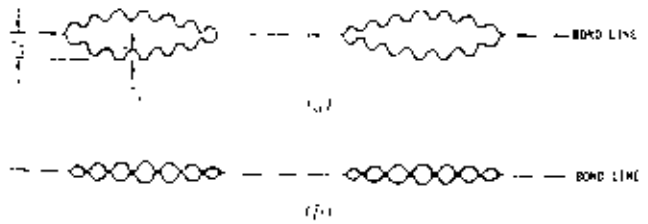

Figure 2.2.8 The long wavelength asperities are flattening during stage I in part (a). In part (b) the welded regions have just achieved contact, and stage II closure begins.

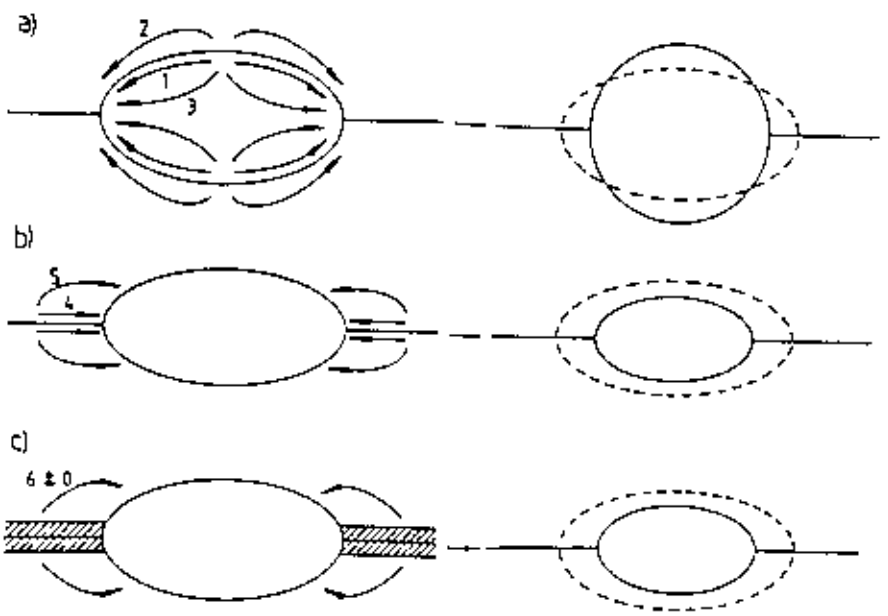

Figure 2.2.9 Routes of the materials transfer: a) surface source mechanisms, b) interface source mechanisms, c) bulk deformation mechanisms.

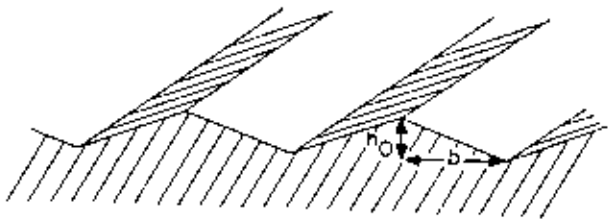

Figure 2.2.10 Derby and Wallach's long triangular section ridges

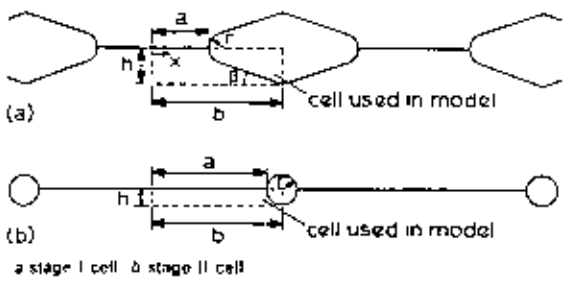

Figure 2.2.11 Contacting surfaces are modelled as small cells (dashed lines) due to assumed symmetry in stage I and stage II.

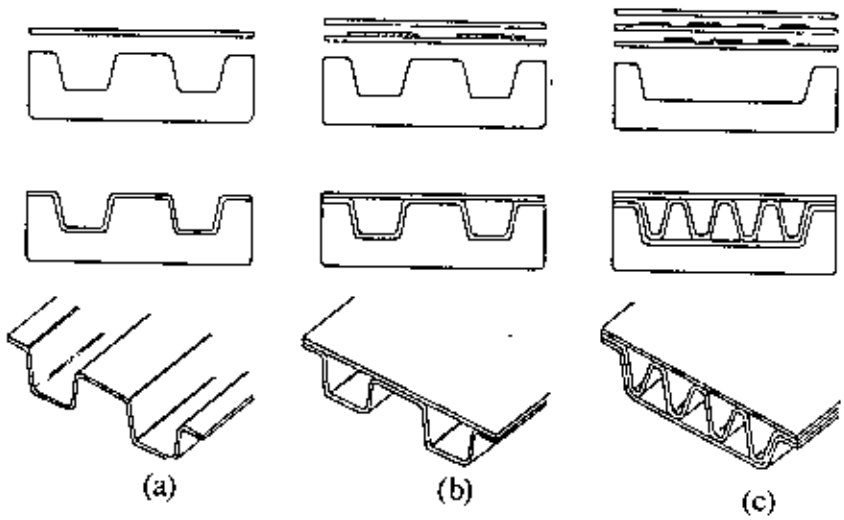

Figure 2.2.12 Principles of (a) Superplastic forming in producing reinforced sheet (b)Superplastic forming - diffusion welding(SPF-DW) in producing stiffened structure (c)SPF-DW in producing sandwich structure.

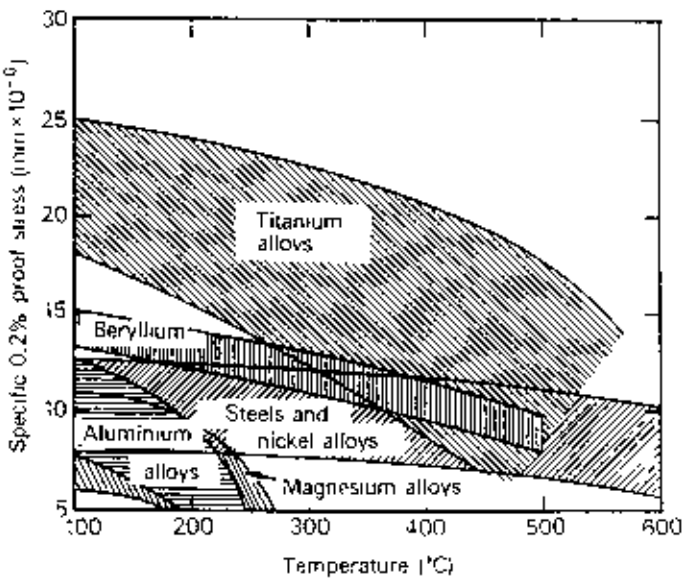

Figure 2.3.1 Relationship of Specific 0.2% Proof Stress (Proof Stress to relative density) with temperature for light alloys, steels and nickel alloys. This shows the superiority of Ti-alloys over the other alloys upto 500°C.

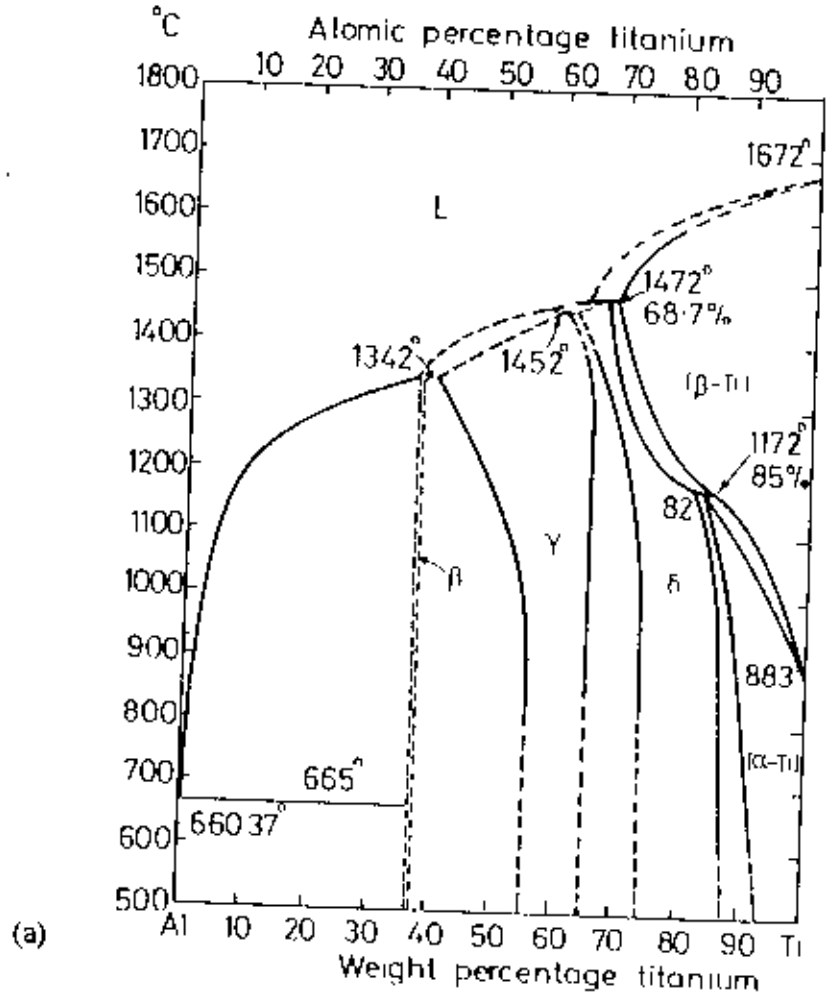

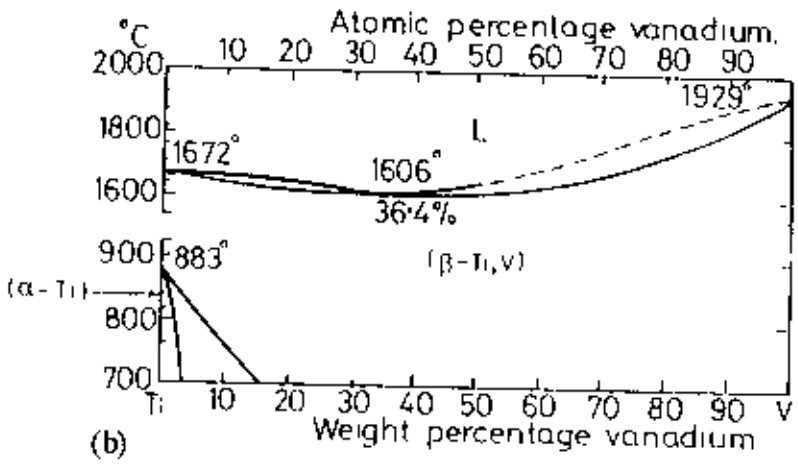

Figure 2.3.2 Phase diagrams: (a)Ti-Al, (b)Ti-V

(a)

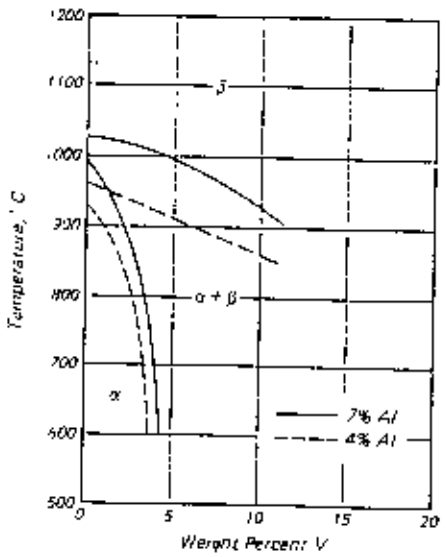

(b)

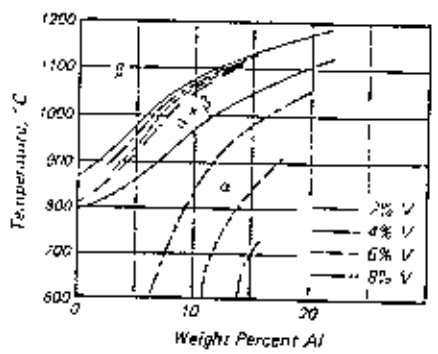

Figure 2.3.3 "Vertical" sections of the Ti-Al-V versus T equilibrium-phase solid (right triangular prism) (a)At 4 and 7 wt% Al, (b) At 2, 4, 6 and 8 wt% V.

Figure 2.3.4 Alternate layer of α(light) and β(dark) in a Widmanstätten microstructure.

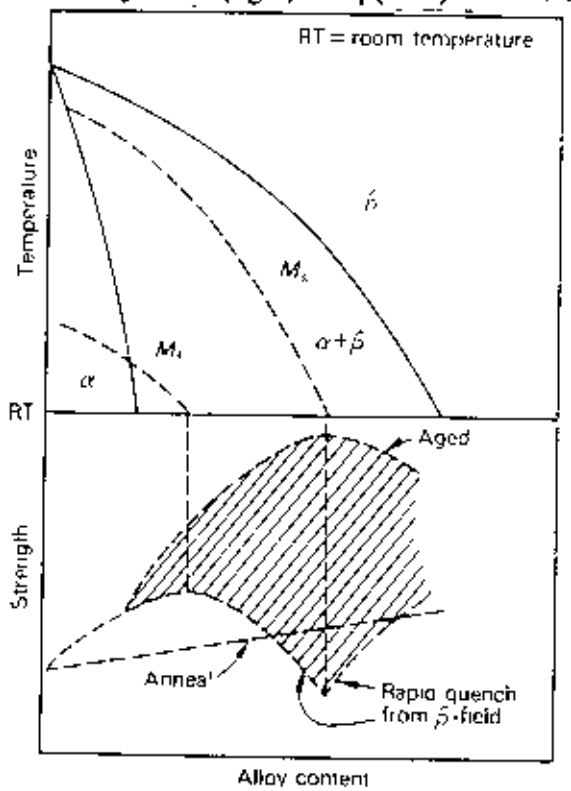

Figure 2.3.5 Schematic diagram for the heat treatment of β-isomorphous titanium alloys.

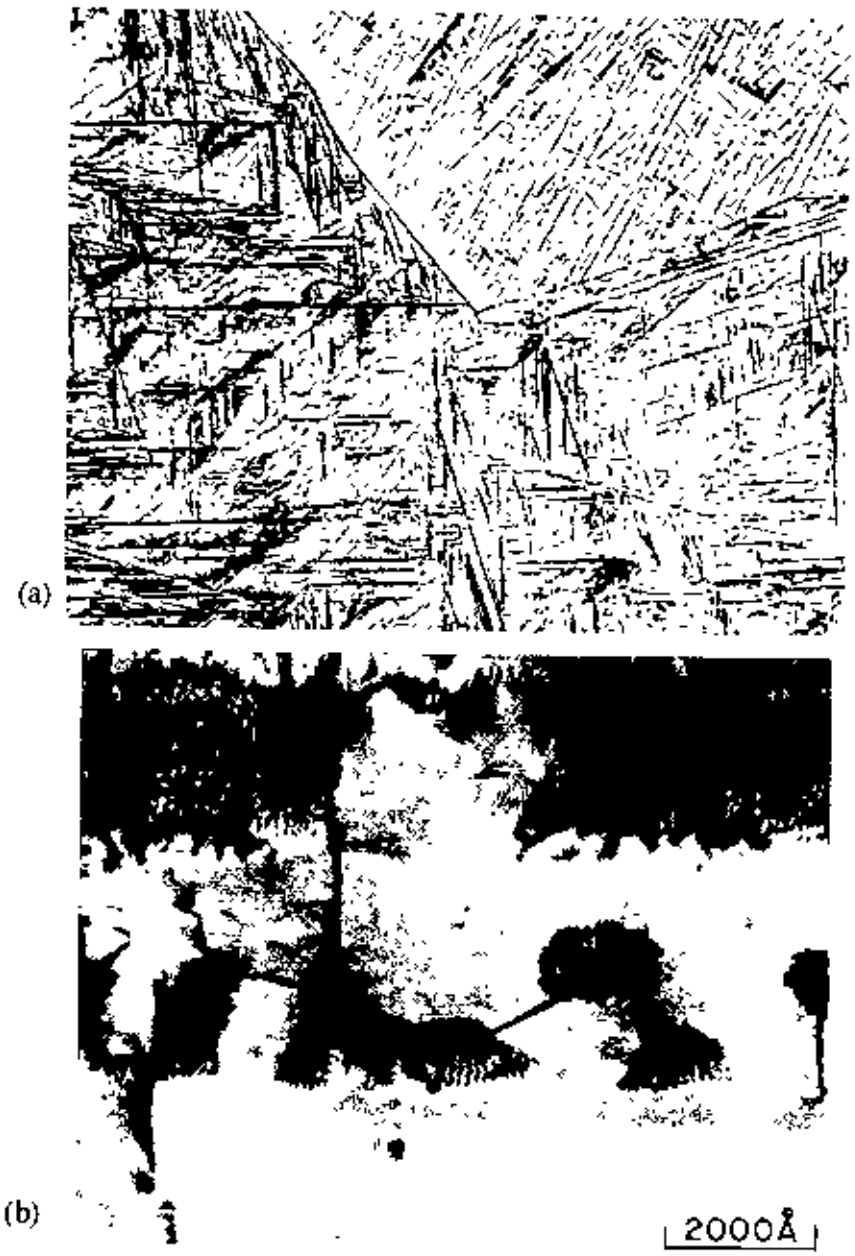

Figure 2.3.6 (a) α′ Martensite in Ti-6Al-4V held above the β transus at 1066°C and water quenched. Prior β grain boundaries are visible, (b) Thin-foiled electron micrograph of the β precipitates that have been formed during the tempering of α′ Martensite in the quenched (from 1100°C) Ti-6Al-4V.

Figure 2.3.7 Microstructure of hot-worked and annealed Ti-6Al-4V.

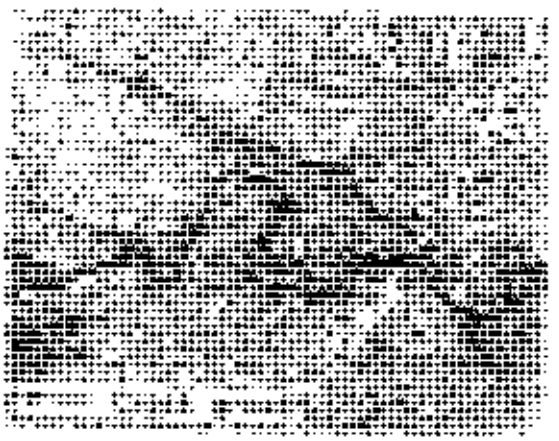

Figure 2.3.8 Branching of fatigue crack within the Widmanstätten packets of the α–lathes.

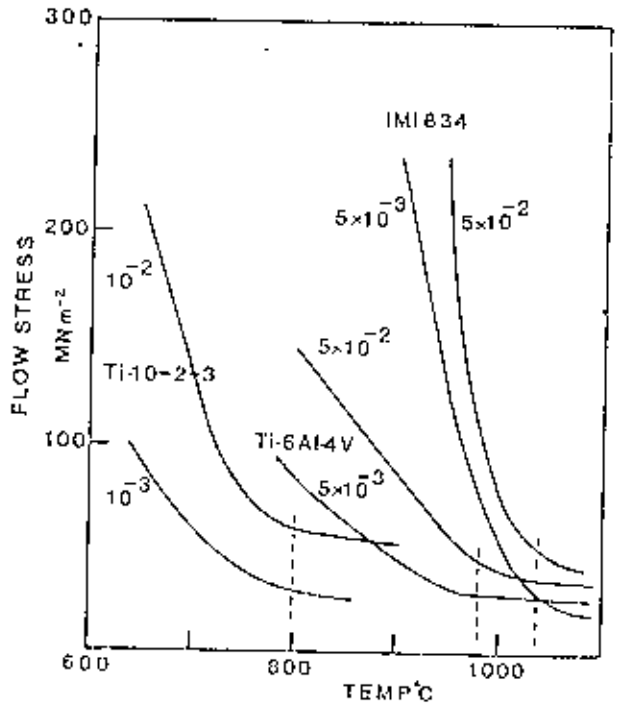

Figure 2.3.9 Flow stress versus temperature for near-β alloys Ti-10-2-3, equiaxed α+β Ti-6Al-4V, and near-α alloy conforming to IMI 834, for two comparable strain rates (indicated for each curve in units of s^{-1}) in each case; vertical dash lines indicate β transus temperature for each alloy.

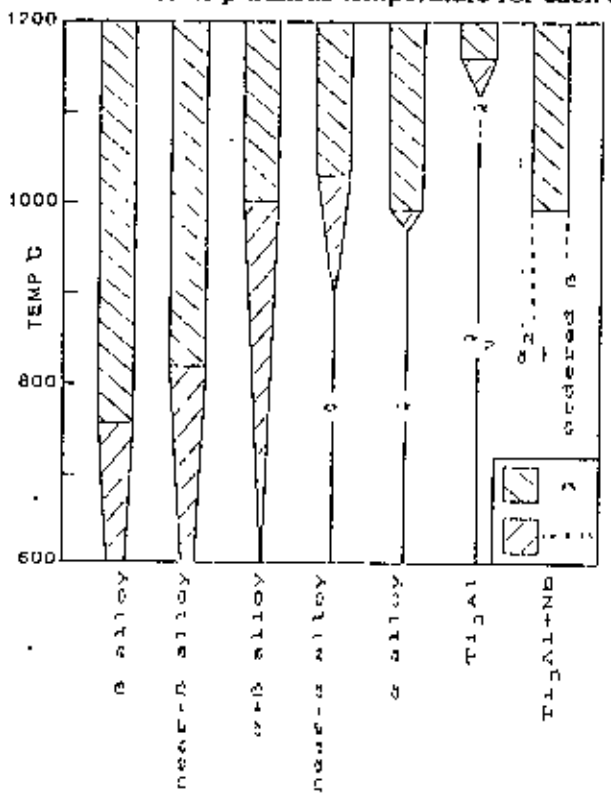

Figure 2.3.10 Temperature ranges for α, α+β, and β phase stability in typical titanium alloys. Amount of β in two phase field is indicated schematically by width of shaded region.

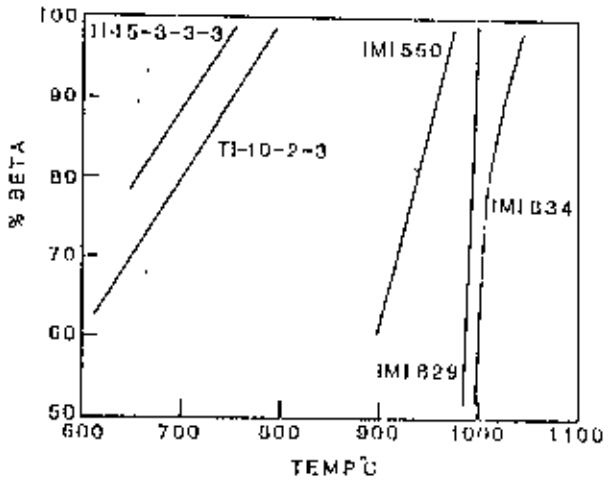

Figure 2.3.11 β approach curves for β(Ti-15-3-3-3), near-β(Ti-10-2-3), α+β(IMI550) and near- α(IMI 829 and IMI 834) alloys; slope of the curves generally decreases with increasing β stabilizer content.

EXPERIMENTAL

3.1 Introduction

In order to carry out diffusion welding experiments, it is required to apply an isostatic pressure on the samples at their optimum superplastic temperatures. The optimum superplastic temperature depends on the phase proportion and the grain size of the alloy at that temperature. Determination of the phase proportion and the grain size at high temperature requires a vertical furnace and for diffusion welding, a special hot isostatic pressure furnace is essential. A vertical furnace has been constructed and materials were characterized using this furnace. A hot isostatic pressure furnace has also been developed and hence diffusion welding experiments were performed.

3.2 Design and fabrication of the furnaces

3.2.1 A vertical furnace

A small vertical furnace, cubic in shape with a vertical chamber, has been constructed from fireclay insulating brick to determine the microstructural condition of Ti-alloys at the desired time and temperature. The outside of the furnace was covered with the asbestos sheet. The heating system is electrical, where SiC heating elements were used. Four heating elements were placed horizontally at the middle of the furnace and encircling the vertical mullite combustion tube. This arrangement creates a small working place in the center of this furnace.

As this is an electrical furnace, it must have an electrical control system to maintain a control power supply for the desired temperature. A thermocouple, placing it's hot junction near the outer surface of the mullite tube at the hot zone, has been integrated to a digital temperature controller. This thermocouple senses temperature and displays that temperature in the digital temperature controller, which controls the electrical supply through a connector according to the set temperature. A step down transformer was also placed to maintain some intermittent voltages over the heating elements which are in series

connection. This produces different current flow through the heating elements at different heating rate. The transformer, connector and the temperature controller were assembled in a panel box.

The temperature fluctuation shown in the display of temperature controller was found near about $\pm 10^{o}C$. Here, the temperature controller senses the temperature from outside of the mullite tube. Another thermocouple was used inside the tube to measure the temperature of the hot zone. By this thermocouple it was found that the temperature fluctuation was reduced to $\pm 5^{o}C$ inside the tube at the hot zone and also temperature was found $10^{o}C$ less than the outer surface. So, it was required to set the temperature $10^{o}C$ upper than the required temperature. This furnace is easy to handle for quenching small specimens from a high temperature. It can be used for microstructural characterization and heat treatment of the alloys.

3.2.2 The Hot Isostatic Pressure (HIP) Furnace

Diffusion welding is generally conducted at the temperature of above $0.5T_m$ (T_m, melting temperature) with applying a moderate pressure equivalent to 5 to 10% of yield strength of the material at the working temperature. For isostatic diffusion welding the pressure on the specimen should be applied from all direction. This type of isostatic pressure can be generated by liquid or gas pressure. Moreover, to protect the specimens from any deleterious effect of high temperature and pressure, the environment within the vessel must be maintained in way that it should neither react with the specimen nor the vessel. In order to provide a neutral environment, high purity argon gas should be used. The gas can be drawn from the cylinder containing 99.97% argon gas supplied by the British Oxygen Company, Bangladesh Limited. As sealing at high temperature is a very difficult task, special considerations were made in designing the pressure vessel. Inconel is one of the best alloy which has high creep and fatigue resistance as well as high toughness. It can withstand the required pressure at high temperature without sudden explosion.

Design and fabrication:

Based on the above requirements a HIP unit was developed with the following two items:

a). a horizontal tube furnace

b). a diffusion welding rig

a) Horizontal tube furnace:

The refractory brick of the furnace body had been designed into two parts: i) internal refractory body containing a center hole for a combustion tube and four holes for heating elements and ii) external refractory encasement.

The internal body was made into three parts, middle of them was designed to create a working chamber of 6 inches length with four SiC heating elements. A hole of 65mm diameter was given through the center of the internal body to place a heavy duty mullite combustion tube. SiC heating elements was inserted around the tubical hole parallel to the center line. The inconel tube can easily be inserted inside the mullite tube. The mullite tube is required to reduce the fluctuation of the temperature around the hole and also to protect the pressure tube from any localized heating due to direct contact between the heating elements and the tube. The external refractory encasement was designed as an annular cylindrical brick to encase the inner bricks as well as for further heat insulation. A small hole was also made through both the external and internal bodies to make access for Pt-Rh thermocouple. The three dimensional view of the body of HIP furnace and the dimensions and all others details of different bricks are represented in Figure - 3.1.

Both the internal and external body were constructed by Super-X refractory materials (45% Al_2O_3) from the Mirpur Ceramics Industry, which can withstand the temperature of around 1500^{o}C. The bricks were assembled and encased by a mild steel cylindrical box to reduce any unexpected violation. The whole furnace was placed only one feet above from the ground on the brick, cement and reinforcing angles construction. The photograph of the assembly is shown in Figure - 3.2.

b) The Diffusion Welding (DW) Rig:

Modification of the previous design:

The first attempt to construct the DW rig was based on the design made by the UMIST laboratory, UK . The DW rig was mainly constructed by a leak proof pressure tube made of inconel alloy, two seal holders with two end caps and a specimen holder. The specimen holder was placed inside the inconel tube to hold the specimen for DW experiments. The dimensions of the inconel tube are as follows:

Overall Length: 608 mm, Outer diameter: 48.48 mm, Inner diameter: 42.48 mm

The total cross-sectional view of the DW rig is shown in Fignre -3.3. External thread were made at the two ends of the tube to tight the end caps. Seal holder was used with the two copper and one brass rings for sealing. The two copper rings, followed by the brass ring were attached to each of the seal holder by means of a screwed component which allowed the end to be sealed. The brass and copper rings were machined from tubular stock and were annealed at 600^{o}C to make them ductile. Copper and brass have 1.5 times thermal expansion coefficient than that of the inconel. During high temperature these copper and brass ring will expand more than the inconel and hence expanded copper and brass rings may produce sealing to the inconel tube. Further sealing was provided by warping teflon tap around the seal holder behind the rings. The dimensions and all others details of the different parts are represented in Figure - 3.4. One end caps was designed for the inlet of the gas and the other one for the inlet of thermocouple (Fig. - 3.4, item 2a and 2b)

The specimen holder consists of several different components made of stainless steel (Fig. - 3.5). Two slots were machined into opposing faces of two round blocks of the specimen holder to hold the specimens and the distance between the blocks was adjusted using two screwed round bars. The two ends of the specimen holder were designed to control the position of the specimen within the middle of the hot zone. The thermocouple was

inserted into the inconel tube by placing it's hot junctions between the two specimens. The contact between the thermocouple and the seal holder was tried to seal by warping teflon tap around the thermocouple.

The seal holder with teflon tape was pushed inside the inconel tube and the end caps were tightened. The assembly was then placed within a single-zone newly constructed horizontal tube furnace. The argon gas was then supplied by copper tubing using a calibrated pressure gauge and a one-way valve, which allowed the gas to be admitted after the inconel tube had attained the test temperature. The interior pressure of the tube was tried to measure by the calibrated gauge located in the system. This modification of the previous design did not give proper leak proofing due to the following reasons:

i) The temperature near the copper and brass rings was near about 150°C. This temperature was not sufficient to expand the rings required to fit tightly inside the inconel tube against the seal holder.

ii) The tapering inside of the inconel tube ends was not accurate for easy going or removal of the seal holder arrangement. This was not possible by the local facilities. Again machining of the ring and seal holder was not at high precision to fit them concentrically inside the inconel tube.

New design:

The above design was fully changed - seal holder with copper and brass ring arrangements had been rejected. At first, scaling was tried by inserting copper(anncaled) gasket between the end caps and the end of the inconnel tube and by tightening the end cap against the tube end. But no better results was achieved for sealing. Manual tightening of the end cap was not sufficient to deform the copper gasket to seal the gap between the periphery of the inconel tube and the end cap. Machine tightening of the end cap might results into scaling. But there was the chance of shearing of the thread to support the high stress involved during deformation of the copper gasket. Furthermore, the machine tightening was not

possible for this HIP furnace. Here, the end cap dimension is larger than the mullite tube. Therefore, one end must be tightened after the insertion of the rig into the mullite tube.

Instead of copper gaskets, teflon gasket was found very effective in sealing the pressure tube. The teflon gasket was fitted in between the end of the tube and the end cap. This gasket has been tighten manually as such that the flexible teflon sealed the interface between the tube and the end cap. Finally the teflon gasket results into proper sealing. The schematic view of the new design is shown in Figure 3.6.

The electrical panel box had been used for the vertical furnace, was also used to control the temperature of the HIP furnace. Here, temperature fluctuation was also $\pm$ 10°C. The temperature in the middle of the pressure tube was measured by the K type Al-Cr thermocouple. The measured temperature was found very close to the reading of the temperature controller, which infect sensed the outside temperature of the mullite tube. The fluctuation of temperature is obvious for this type of furnace as the heating source is employed outside of the working chambers.

3.3 Characterization of the materials properties

3.3.1 As-received microstructure

IMI-325 and IMI-318 alloy sheets were cut into 10mm X 10mm pieces to examine the as-received microstructure of materials. These were mounted in resin and polished by standard metallograpic techniques and etched with standard Kroll's reagent containing 88%H_2O, 10% HNO_3 and 2%HF. The polishing and etching processes were repeated several times. After a long trial when the microstructure had been revealed, photographs were taken. The average grain size was measured by mean linear intercept method.

3.3.2 Heat treatment of IMI-325 alloys

The IMI-325 alloy having nominal composition (at%) of Ti-3Al-2.5V was received in the form of superplastic grade sheet of thickness 1mm. To measure the volume fraction of the

β phase proportions with temperature, the alloy was heat-treated at 820°C to 940°C. This involved 30 minutes holding followed by water quenching with the help of the vertical furnace. After metallographic preparation the volume fraction of the β- phase proportion was measured by using Image Analysing system. The variation of average grain size with temperature was also measured.

3.3.3 Heat treatment of IMI-318 alloy

The volume fraction of β-phase with temperature for this alloy was measured after heat-treatment. This involved heating the samples in the temperature range of 860°C to 940°C for holding 30 minutes followed by water quenching. The as-quenched samples were prepared for microstructural analysis and % of β- phase was measured. The average grain size for this alloy was also measured for the temperatures of 860°C to 940°C and holding times of 15 minutes to 2 hours by the same procedure as described for the IMI-325 alloy

3.4 Diffusion Welding

To preserve the microstructural stability of the IMI-325 and IMI-318 alloys, welding was carried out at temperatures as close as possible to those at which each material contained 30-50% β phase volume fraction. The welding temperature range was investigated for both the alloy through the microstructural characterization. And accordingly, welding experiments were carried out for the temperature range of 840°C - 880°C for similar couple of IMI-325 and 840°C - 860°C for dissimilar IMI-325 to IMI-318 where the microstructures of the both materials were substantially unaffected. Commercially one hour welding time and 2.1MPa pressure for industrial titanium alloys (such as IMI-325 and IMI-318) have been widely adopted. In the present work, pressure was varied form 2.1MPa (300 Psi) to 2.5MPa (360Psi) for the welding time of 1/2 hour and 1 hour.

3.4.1 Preparation of the specimens

For diffusion welding studies, blanks measuring 88mm x 26mm for IMI-325 and IMI-325 to IMI-318 were cut from the sheet materials. The IMI-325 and IMI-318 were chemically

cleaned to achieve same degree of roughness. After the surface preparation, pairs of blanks were electron beam welded around their peripheries to form a single DW couple.

3.4.2 Diffusion welding procedure

The single DW couple was placed loosely between the slots provided in the specimen holder. The clearance was made to allow the differential thermal expansion of the titanium specimen and the stainless steel specimen holder. The specimen holder with the specimen was put inside the inconel pressure tube. The pressure tube was closed by tightening the end cap with teflon gasket placing it in between the periphery of the tube and the cap. The tube was then inserted inside the horizontal HIP furnace and connected to the high purity argon gas cylinder.

To start the welding process, the furnace was heated upto the welding temperature. In the present study, the welding temperature was used in the temperature range of 840°C to 880°C. When the required temperature was reached, the interior of the tube was pressurized. This was carried out by filling the tube with argon gas until the required pressure was obtained.

The pressure was read continuously from the calibrated gauge located between the tube and the gas cylinder. Welding pressure and temperature were kept constant during the welding procedure. Finally, after heating the assembly for the desired welding time the furnace was switched off. The pressure was released and the gas supply was disconnected, then the assembly with the specimen was cooled in the furnace to room temperature.

Mention may be made here that one experiment was done for zero holding time where after attaining the required temperature pressure was developed and released momentarily. And then the furnace was switched off.

3.4.3 Optical Microscopy

Conventional light microscopy was used to obtain information about the microstructure and weld line conditions. Three specimens were cut carefully from three different position of the welded sample by the diamond cutter. During cutting, a copious flow of water was maintained. The diffusion welds were examined by taking the transverse sections in order to detect any interfacial voids, local grain structure and the quality of the weld using the Shimutzi Microscope. The samples were prepared by standard metallographic techniques. Etching and polishing were repeated a few times until a good microstructure was revealed. After examining the weld line thoronghly, photographs from different position for each sample were taken using photomicroscope.

3.5 Post - heat treatment of previously welded samples

Diffusion welded samples of two dissimilar titanium alloys (such as IMI-318 and super $\alpha 2$) which were welded in UMIST laboratory were solution-treated from the temperatures of 830°C to 920°C for different holding times (1hour to 2hours). Some of them were annealed in a furnace and others were water quenched. Water quenched samples were aged at different temperatures (600°C to 700°C) for time between 5 hours to 13 hours. All the samples were then polished using standard metallographic techniques and etched with the standard Kroll's reagent.

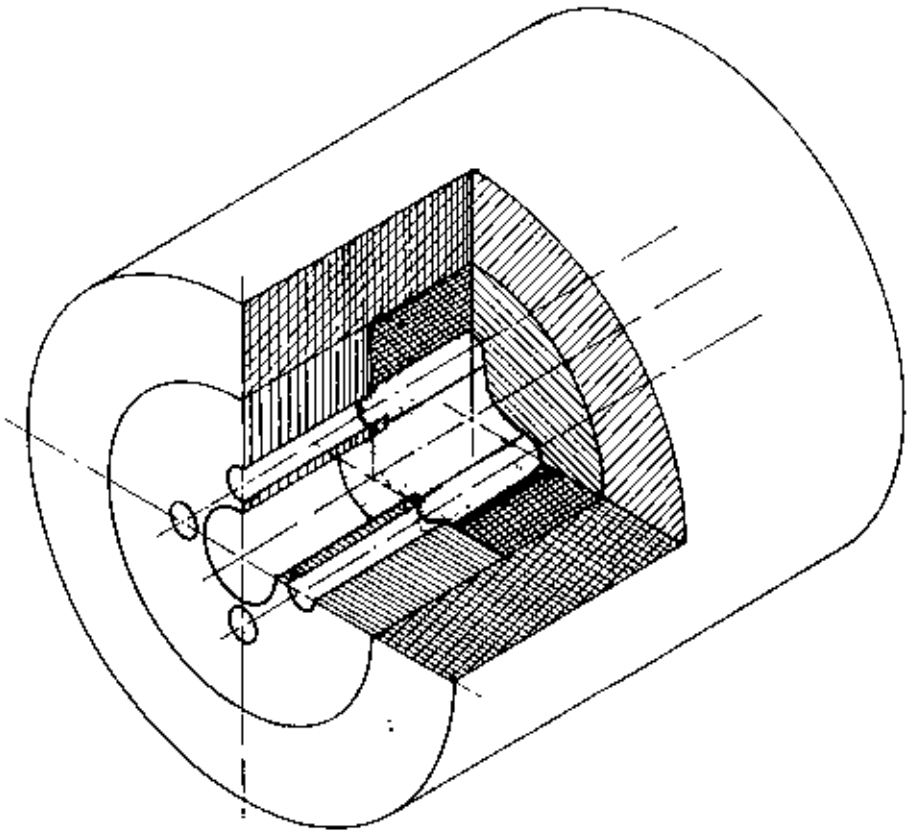

Figure - 3.1 a ' - The three dimensional view of the HIP furnace body

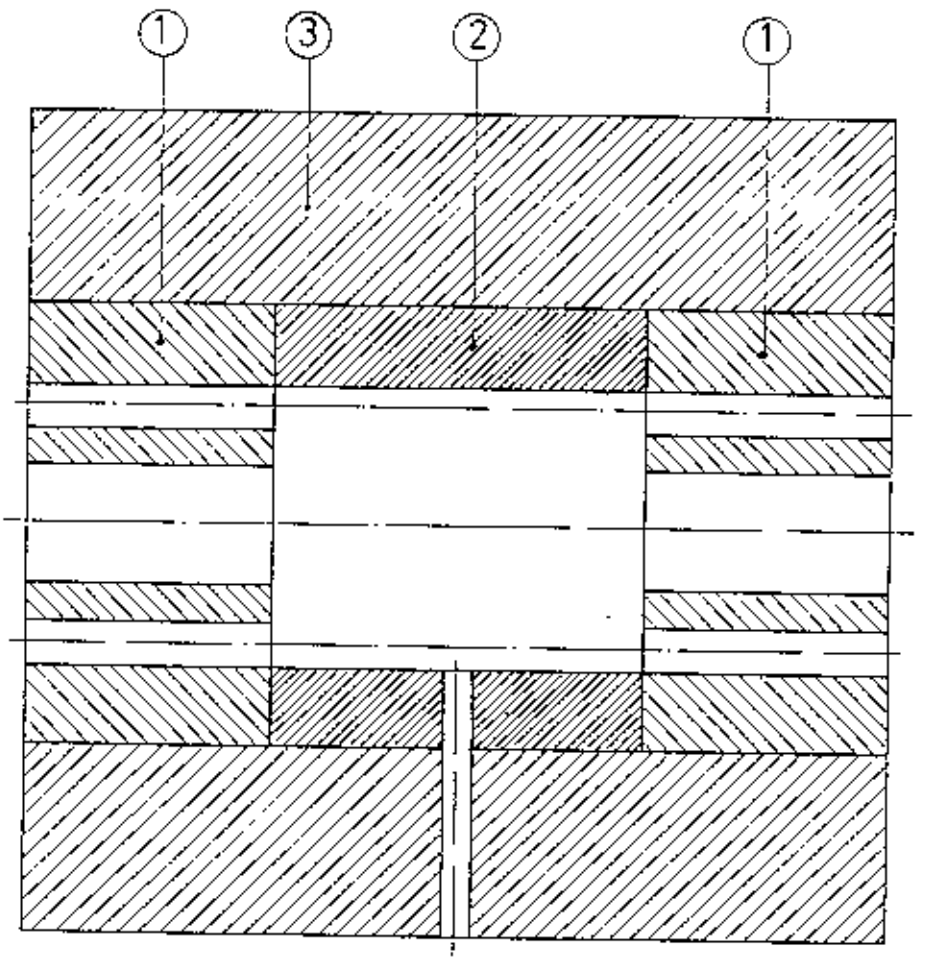

Figure - 3.1 b : - The individual refractory bricks of the HIP furnace

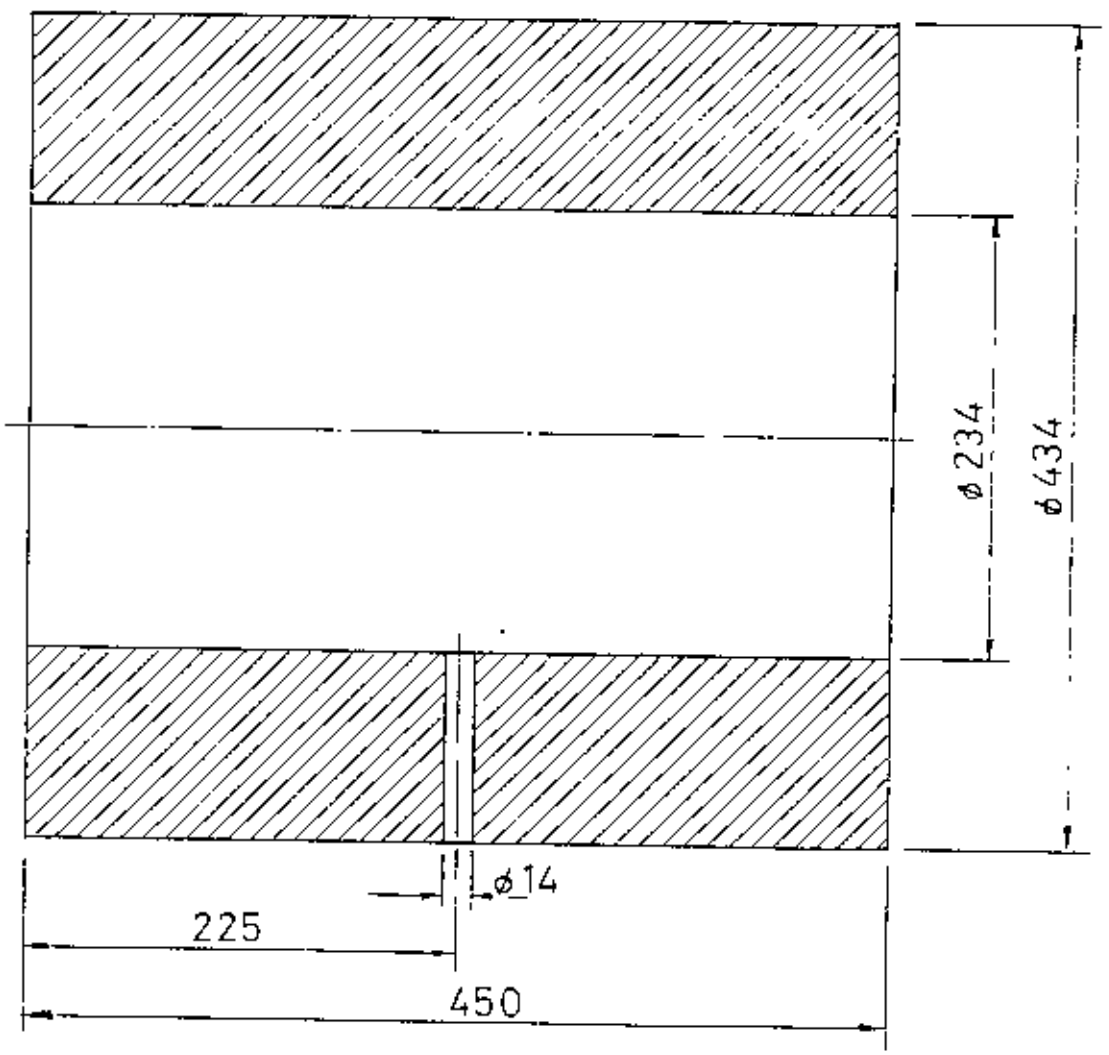

Figure - 3.1 b : - The individual refractory bricks of the HIP furnace (continued)

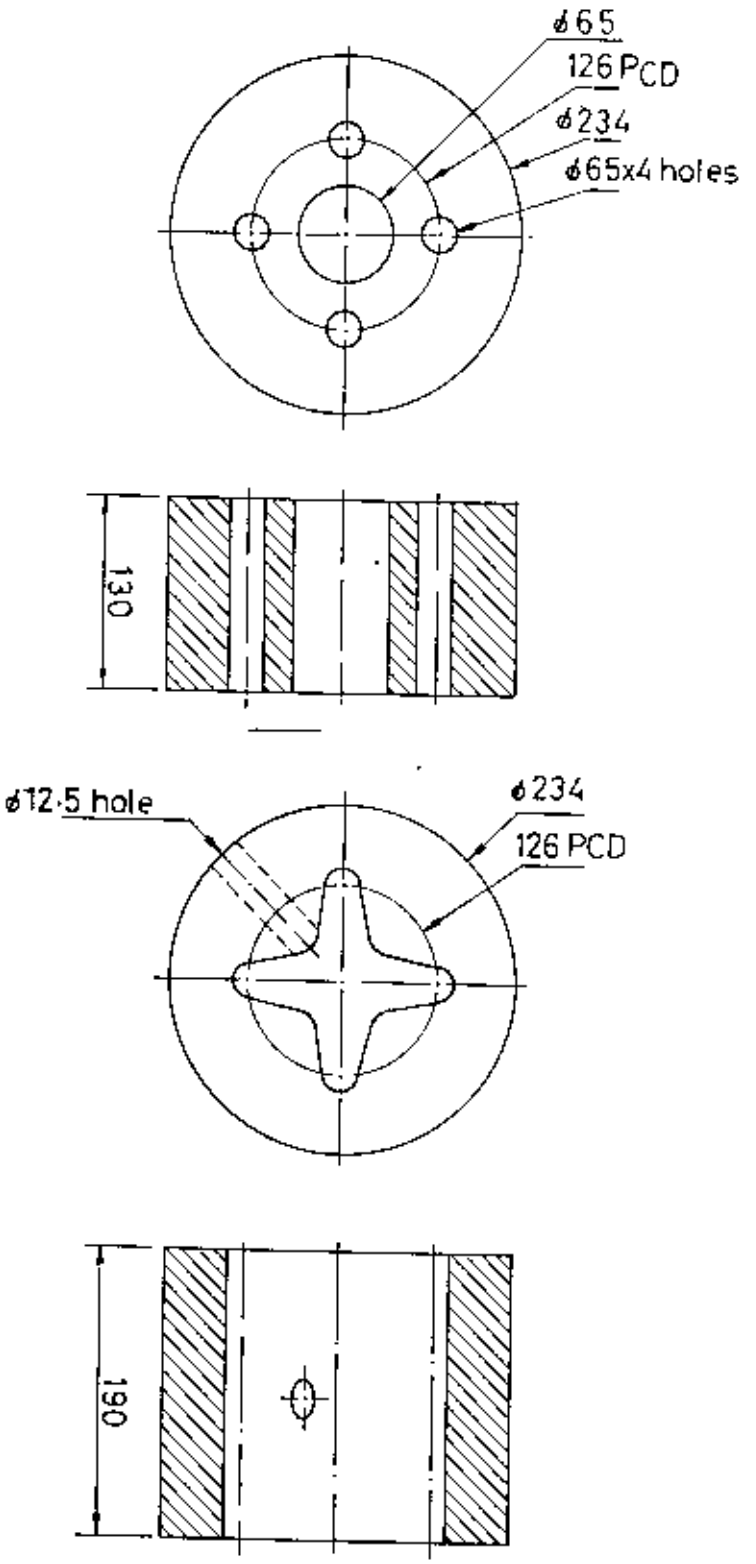

Figure - 3.1 b : - The individual refractory bricks of the HIP furnace (continued)

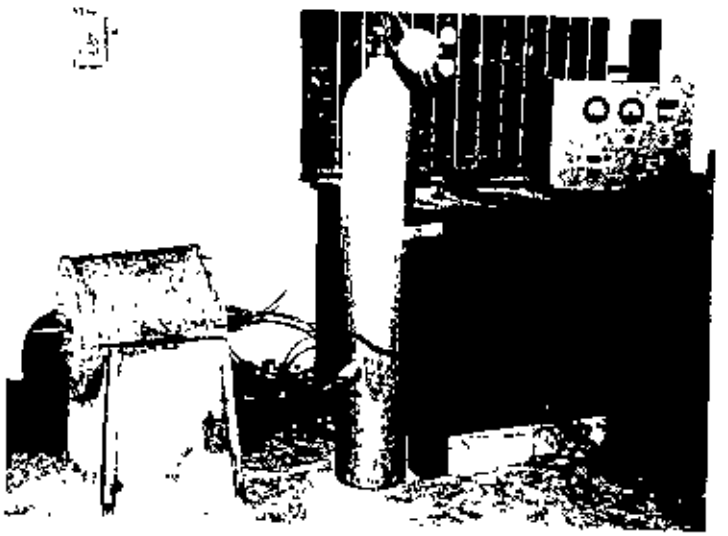

Figure- 3.2 : - The photograph of the HIP furnace assembly.

Item no.	Item name	Mat.	Qty.	Item no.	Item name	Mat	Qty
1	Inconel tube	Inconel alloy	1	2.a.b	End cap	Steel	2
3	Seal clamp	"	2	4	Seal holder	Inconel alloy	2
5	Ring	Copper	4	6	Ring	Brass	2

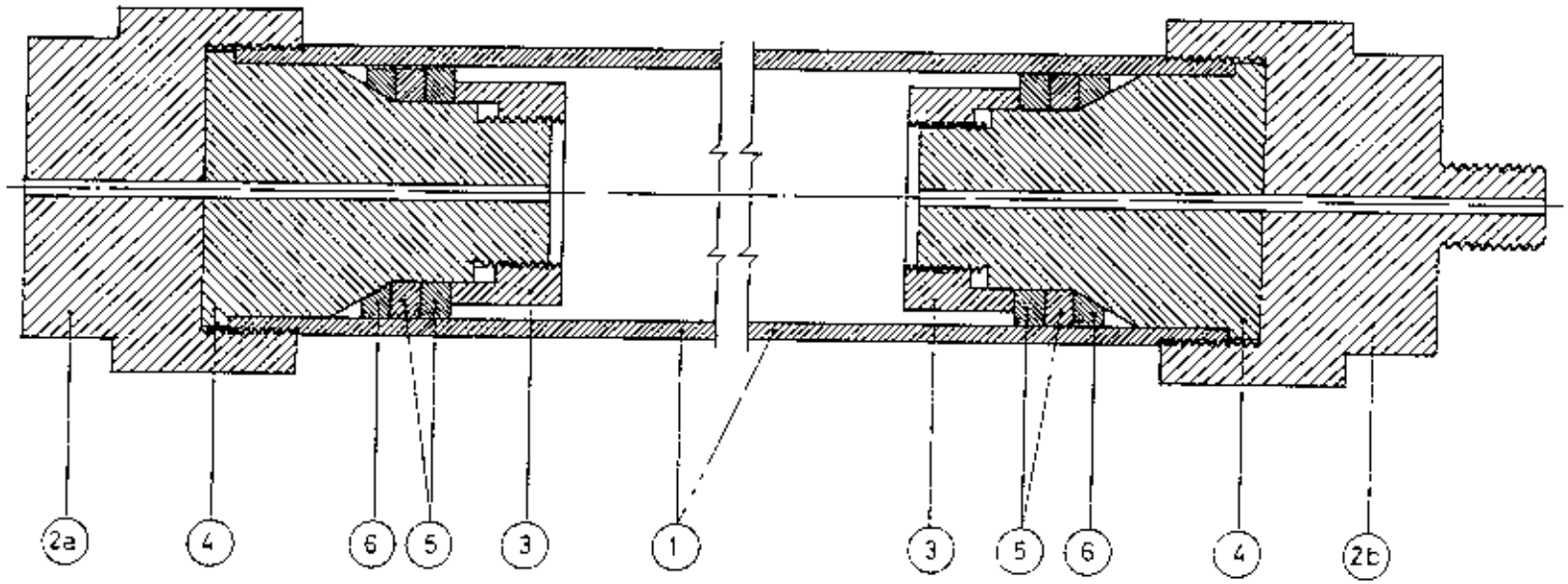

Figure- 3.3 - The total cross sectional view of the diffusion welding rig

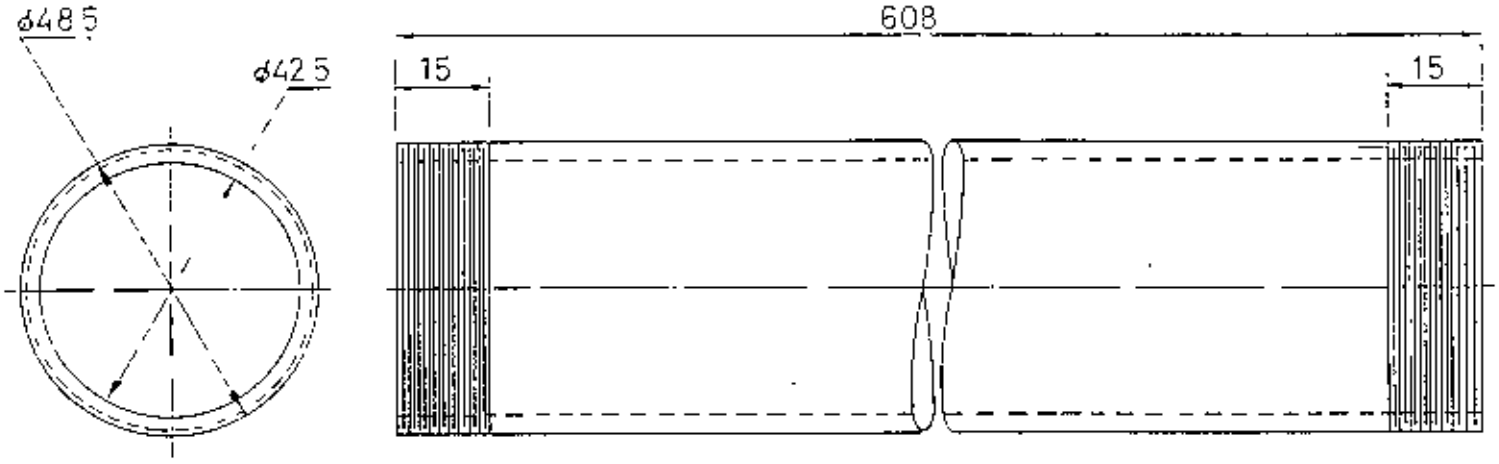

ITEM :- 1 . INCONEL TUBE

Figure- 3.4 :- The details of the individual parts of the diffusion welding rig.

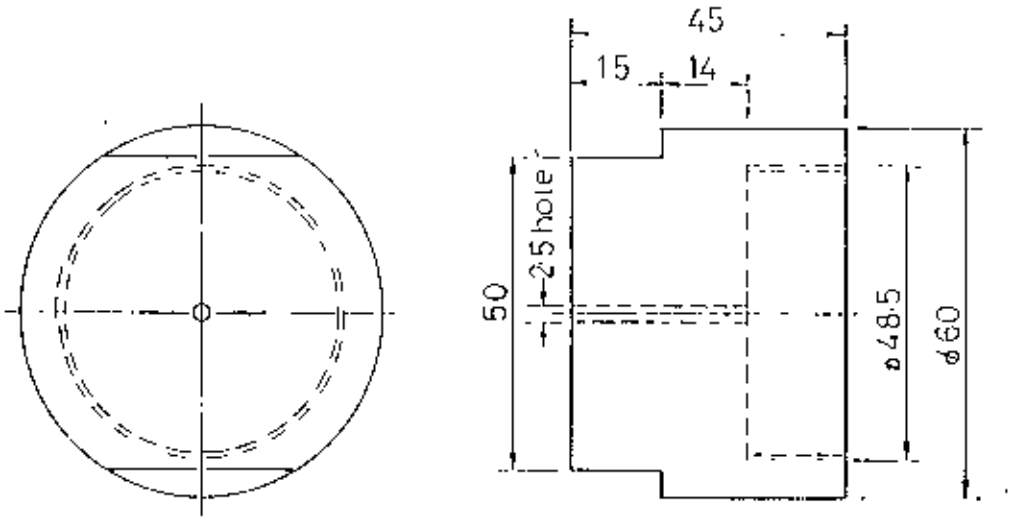

ITEM - 2a END CAP

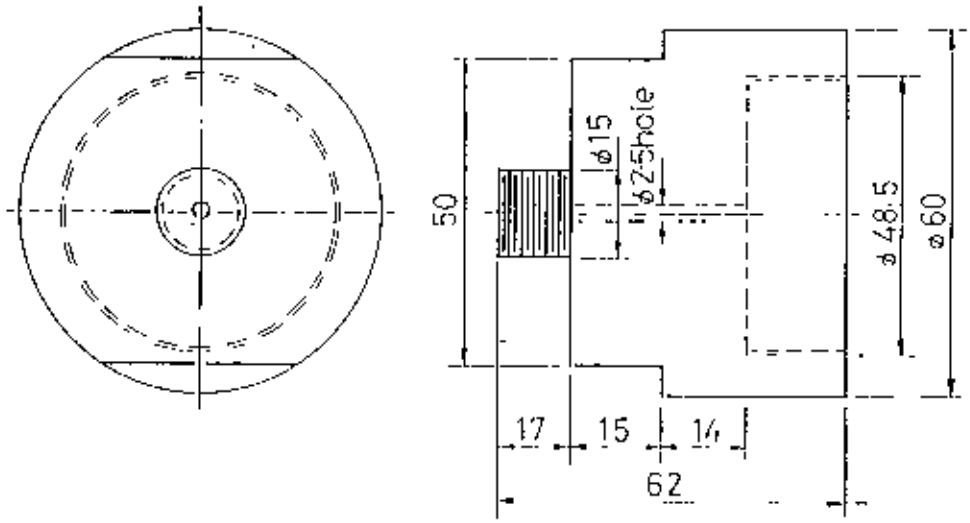

ITEM - 2b END CAP

Figure- 3.4 :- The details of the individual parts of the diffusion welding rig

(continued)

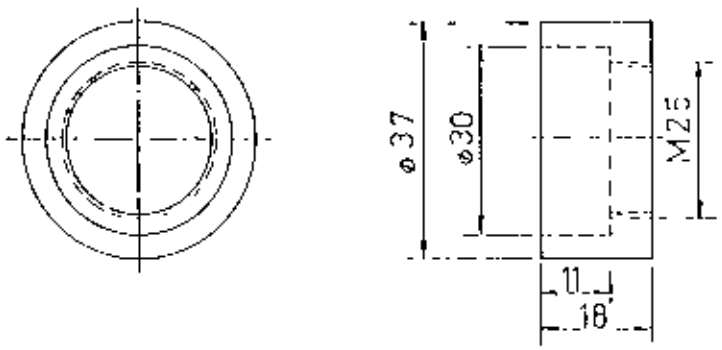

ITEM :-3 SEAL CLAMP
2 Nos

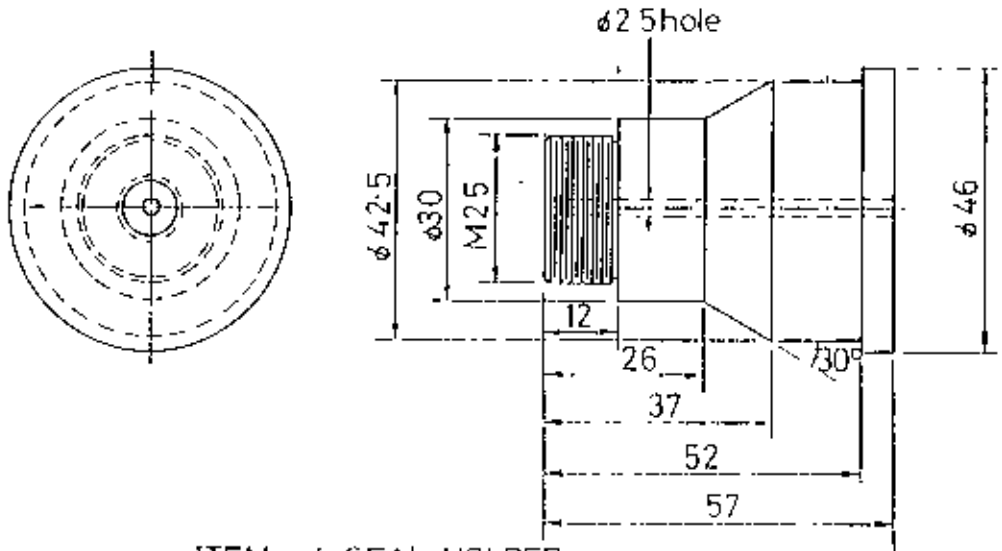

ITEM :-4 SEAL HOLDER
2 Nos

Figure- 3.4 :- The details of the individual parts of the diffusion welding rig (continued).

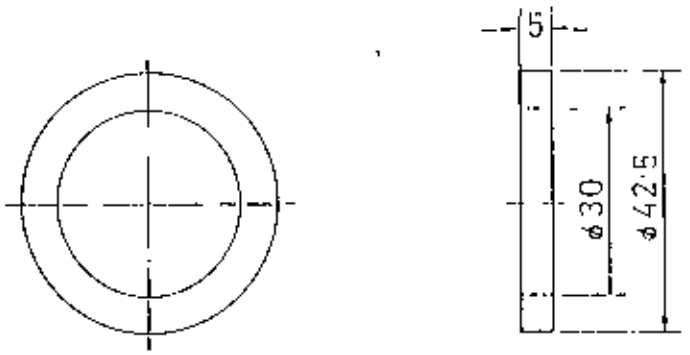

ITEM :- 5 COPPER RING
4 Nos

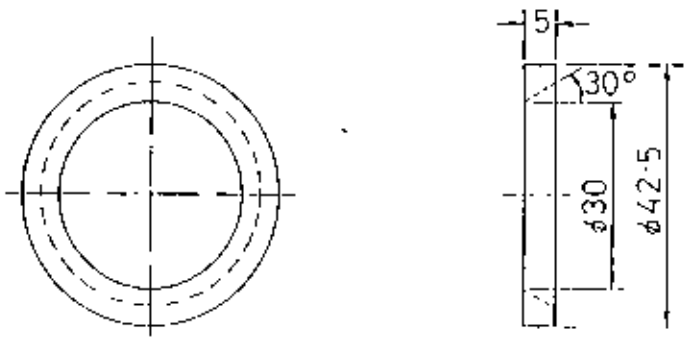

ITEM :- 6 BRASS RING
2 Nos.

Figure- 3.4 :- The details of the individual parts of the diffusion welding rig (continued).

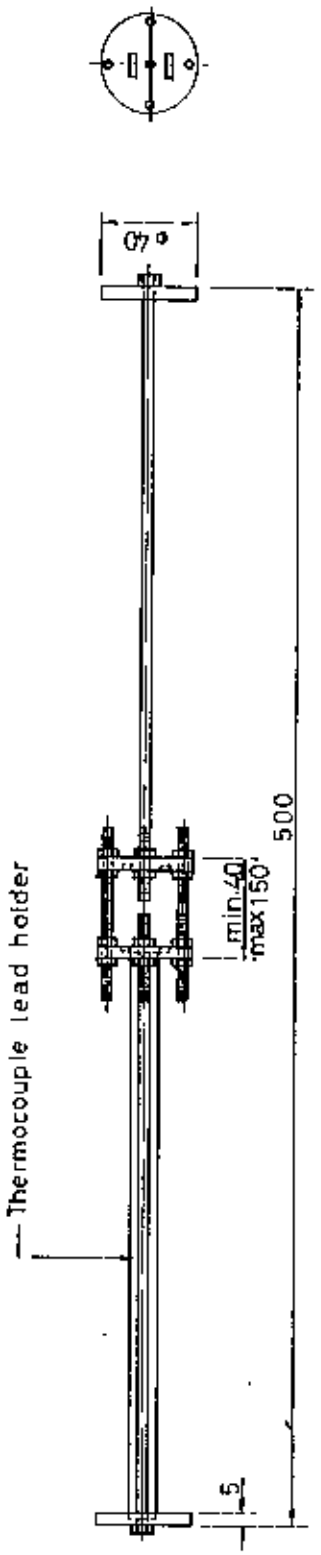

Figure- 3.5 :- The front view of the specimen holder

Item no.	Item name	Mat.	Qty.	Item no.	Item name	Mat.	Qty.
1	Inconl tube	Inconel alloy	1	2	End cap	Steel	1
3	Endcap	Steel	1	4	Teflon gasket		1
5	Teflon gasket		1				

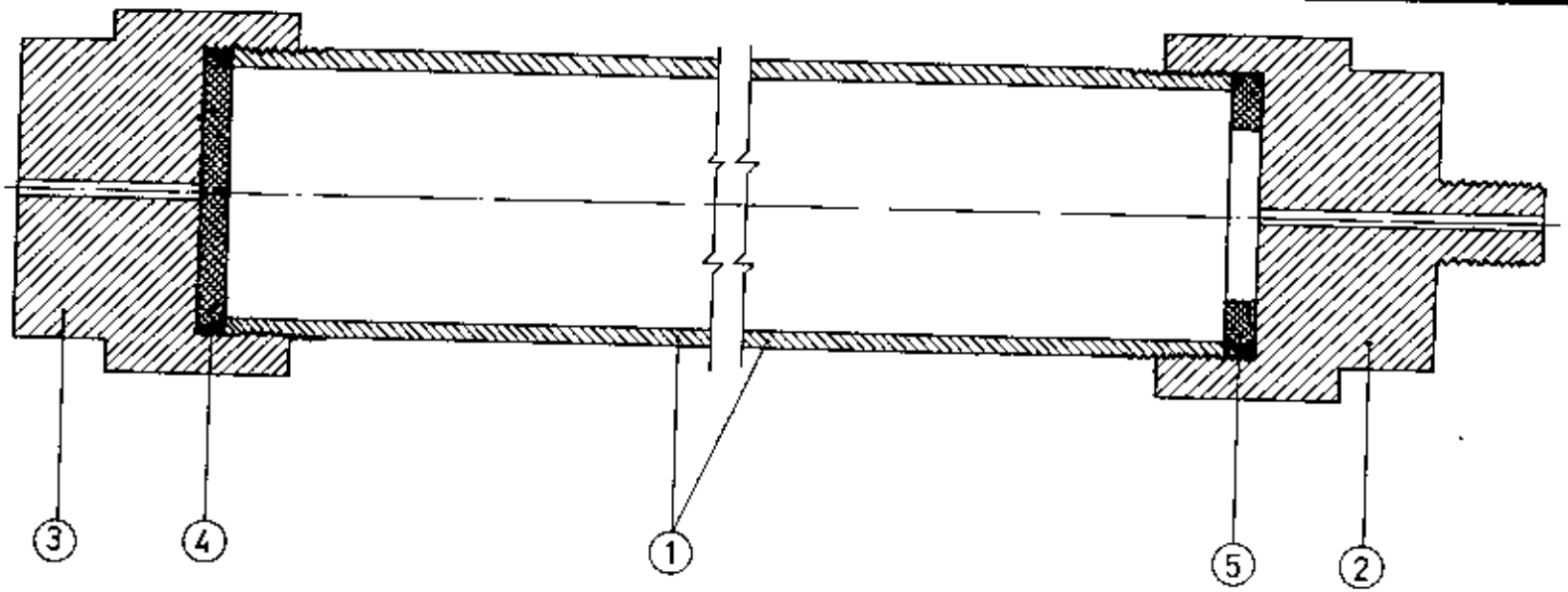

Figure- 3.6 :- The ultimate design of the seal holder.

4. RESULTS AND DISCUSSION

4.1 Introduction

The aim of the present work was to develop a hot isostatic pressure (HIP) furnace and carry out diffusion welding experiments for titanium alloys using this furnace. The development of the HIP furnace is a real achievement of the present work. The main focus of the present work was to produce a sound weld between two sheets of IMI-325 and dissimilar sheets of IMI-325 to IMI-318. An assessment of the quality of welds produced was made on the basis of metallographic examination. In addition, post heat-treatment of diffusion welded samples of dissimilar alloys (welds between IMI-318 to titanium aluminide) has also been carried out to eliminate the microstructural inhomogenities at the interface region.

4.2 Diffusion welding of IMI-325

4.2.1 Materials

The microstructure of the as-received samples of IMI-325 had a very fine deformed and banded structure of α and β phases (Figure - 4.1). Such types of microstructure was formed during cold rolling required to produce 1mm thin sheet. The average grain size of the as-received materials was measured about 3 μm. This grain size is the average of the three dimensional flat surface, long transverse and short transverse sections.

Figure - 4.2 shows the microstructures of water quenched samples of IMI-325 at 840^{o}C and 910^{o}C for 30 minutes. The variation of β phase with temperature is shown in Figure 4.3. It is clear that after 880^{o}C, the percentage of β phase proportion was increased rapidly. The fine grain size required for superplastic deformation was found to be preserved below the temperature of 880^{o}C. With increasing β phase proportion the grain size also tended to be increased abruptly (Fig.- 4.2b). This was due to the higher diffusion rate in b.c.c. β phase[35]. The curve showing the β phase proportion versus temperature reached to 100% β at 920^{o}C. It can be concluded that the β transus

temperature of IMI-325 is about 920°C. For near α and α/β titanium alloys, diffusion welding is usually carried out at temperatures close to those for optimum superplastic behaviour, when the materials contain less than 50% volume fraction of β phase and the average grain size is less than 10 μm. Therefore, diffusion welding temperature for this alloy has been chosen in the range of 840°C-880°C.

4.2.2 Metallography of the diffusion weld of IMI-325

The conditions required to produce sound weld between two sheets of as-received and chemically pickled IMI-325 have been examined by optical microscope. Welding was carried out between the temperature of 840°C to 880°C and the pressure 2.1 MPa (300 Psi) to 2.5 MPa (360 Psi) for 1 hour.

Figure 4.4 a and b show the microstructures of the welded sample of IMI-325 made for 1 hour at 840°C + 2.1 MPa and 840°C + 2.5 MPa respectively. Distinct identification of the weld line with voids (in Figure 4.4 a) supports the assumption of the elliptical voids by the previous model for the theoretical calculation of welding time[11]. The voids are discontinuous and irregular in shape. Discontinuous distribution of the voids in the weld line may be due to irregular contact of the peak to valley and/or peak to peak of the surface asperities between two original surfaces. Detailed examination of the weld line in the microstructure has shown that there is still ~30 percent voids to be removed. The contact point between peak to peak or peak to valley of the surface asperities are the nuclei of the welding process. The peak to valley contact is more favorable than peak to peak contact for speedy bonding rate. However, the number of the contact increases as the pressure is increased. But where the long wave lengths of the two opposing surfaces are in peak to peak contact, there has the least possibilities of joining and require higher pressure for welding[15]. The effect of pressure has been proved by the welding experiment done under the condition of 840°C + 2.5 MPa + 1 hr and the microstructure is shown in Figure 4.4 b. The figure reveals that the amount of voids have been reduced to less than 5 % of the total bonded area. Both the experiments were carried out at the same temperature and time but

the pressure was varied. The difference in the bonded area and the void shapes between the Figure 4.4 a and b may be due to the higher applied pressure (2.5 MPa) than the first welding.

The pressure has major effect on the welding mechanism at least on it's first step i.e. instantaneous plastic collapse of the surface asperities[1]. The more the pressure, the more asperities collapse plastically and hence the more welded area would be achieved instantaniously. The welding temperature of this alloy was maintained within the range of it's superplastic deformation temperature. Therefore, the pressure also increases the rate of superplastic flow or creep flow which enhances the rate of voids closure. The third mechanism of diffusion welding is the stress directed atomic diffusion which is mostly dependent on the temperature and time[2,3].

To evaluate the individual effect of the instantaneous plastic collapse from the among three mechanisms, a diffusion welding experiment has been carried ont at 860°C and 2.5 MPa applied pressure for zero holding time. The microstructure of the welded sample is shown in Fignre 4.5. It was found that ~25% of the total area has been welded by instantaneous plastic collapse of the surface asperities. If the applied pressure would be more than 2.5 MPa, the percentage of welded area due to instantaneous plastic collapse might be higher than 25%, reducing total time for diffusion welding.

Figure 4.6 a and b show the microstructures of the welded sample of IMI-325 made for 1 honr and 2.1 MPa at 880°C and 860°C respectively. The microstructures of Figure 4.6a shows a very few isolated pores within the grains lie on the original weld line. This may be dne to rapid grain migration and grain growth in this temperature (880°C) remaining the pores isolated in bulk of the grains. These isolated pores can only be eliminated by volume diffusion which will take longer time.

Sound welding has been produced at the welding condition of 860°C + 2.1MPa + 1hr (shown in Fig 4.6b). This microstructure shows that no pores lie on the weld line. Precise microstudy of the weld line shows that grain boundary decoration in the weld line

has been found in some areas whereas most of the weld line has not been detected due to grain migration. From the above experiments it can be concluded that 860°C + 2.1MPa + 1hr is the best parameter for the welding of IMI-325.

4.3 Diffusion welding of dissimilar titanium alloys

4.3.1 Materials

As-received IMI-318 had also a very fine deformed microstructure of α and β phases (Fig 4.7). This material was also heavily cold rolled to produce 1.6 mm thick sheet . The grain size in the as-received condition was near about 5 μm.

Figure - 4.8 shows the microstructures of IMI-318 after holding at the temperature of 880°C and 940°C for 30 minutes and followed by quenching in the water. From the microstructures it is clear that 40-50% β phase exists at the temperature range of 860°C-920°C. The amount of β phase increases as the temperature increases. The variation of the volume fraction of β phase with temperature is shown in Figure 4.9.

During welding between these two dissimilar titanium alloys (IMI-325 and IMI-318), the overlapping temperature range for the superplastic deformaiton of these alloys has been considered. This overlapping temperature is found to be 860°C-880°C. So, 860°C-880°C is the optimum temperature for diffusion welding between IMI-325 and IMI-318.

4.3.2 Metallography of the diffusion weld between IMI-325 to IMI-318

Diffusion welding experiments for IMI-325 to IMI-318 have been carried out under the conditions of 840°C at 2.1 MPa for 1/2 hour and 860°C at 2.1 MPa for 1 hour. Figure 4.10 shows the microstructure of diffusion weld between IMI-325 to IMI-318, using welding conditions of 840°C and 2.1 MPa for 1/2 hour. From the microstructure it is clear that welding has not been fully completed. Although the pressure is sufficient for the instantaneous collapse of the asperities of both the alloys and creep/superplastic flow, but due to the lower temperature as well as relatively less time, the planner array of voids

could not be removed through diffusion. If a little bit of higher temperature than 840°C and/or sufficient time were allowed then the grain boundary and volume diffusion could result into a sound weld. The microstructure of the welded samples for the condition of 860°C at 2.1 MPa for 1hour has shown in Figure 4.11. The microstructure is free from any voids on the weld line . Moreover, it is clear from the Figure-4.11 that the IMI-325 to IMI-318 weld interface does not have any significant microstructural difference from the parent structure.

4.4 Post Heat treatment of Diffusion Weld between IMI-318 to Titanium Aluminide

Figure 4.12-a and 4.12-b show the microstructures of diffusion welds between IMI-318 to titanium aluminide alloys using welding conditions of 940°C with 10 MPa for 1hour and 920°C with 10 MPa for 1hour[2,45]. Examination of the weld interface prior to etching showed that the welds formed were free from interfacial porosity, indicating that potentially sound weld had been formed. Both the microstructures of the weld interface seen in Figure 4.12 show a narrow diffusion-affected interface region (DAIR) ranging from ~15-25 micron width in the IMI-318 side near the weld line. This weld zone is devoid of equiaxed alpha grains into transformed beta, revealing distinct fine alpha platelets of about one micron wide . The thickness of this diffusion zone is clearly increased as the welding temperature is increased from 920°C to 940°C (Fig.- 4.12 a and b)

EDX microanalysis for the specimen welded at 940°C with 10MPa for 1 hour is shown in Figure 4.13[2, 45]. It can be seen that the profiles are serrated and this reflects the fact that the measurements are being taken on duplex microstructures which are present in the three regions of interest, i.e. two parent materials and the transformed interface region. The diffusion profile shows that a significant amount of Niobium (Nb) diffuses across the weld interface from titanium aluminide to IMI-318, as well as some diffusion of Molybdenum (Mo). Both of these elements are β stabilizers. At the welding

temperatures, the equilibrium Nb concentration in the beta phase dropped down to about one-half the concentration at room temperature[46]. Excess elemental Nb and to a lesser extent, Mo from the titanium aluminide then become available to diffuse into the neighboring α_2 particles and eventually across the interface into the IMI-318 to decrease the concentration gradient.

Build up of β stabilizers at the welding temperatures causes a local suppression of the β transus and promotes the dissolution of the equiaxed α particles in the IMI-318 next to the interface leading to a fully β phase. Attempt had been made to destroy the transformed interface region of acicular α-phase which had been appeared after furnace cooling during diffusion welding. The welded specimens were first solution treated at 920°C, 900°C, and 880°C for 2 hours, 1.5 hours and 1 hour and annealed to spherodize the platelet α. But the microstructures showed little spheroidization effect. Previous thin platelet only got thicken. (Fig-4.14) Then it was thought that the α platelet were produced from the fully β-grains of DAIR. Once β transformation occurred for Ti-alloys then slowest cooling would not produce equiaxed α . So, whether β-transus crossed or not during the post-heat treatment (solution treatment followed by annealing) the α could not be removed. In order to remove this Widmanstätten- α, there is no way other than quenching above the β-transus to dissolve α platelet and aging (to produce equiaxed α), at the temperature where appreciable diffusion could occur. The diffusion weld specimen (welded at 940°C, 10MPa and 1hour) is solution treated at 900°C, 860°C, and 830°C for 2 hour and then water quenched to find out the β transus temperature range of DAIR. It has been determined that the β transus temperature of the DAIR has gone down to 900°C which is lower than that of the both parent alloys. Figure 4.15 shows the microstructure of the diffusion welded specimen which is solution-treated at 900°C for 2hour and then water-quenched. The DAIR of this specimen fully consists of retained β-phase. The solution treated and quenched diffusion weld specimen is aged at 700°C for 5 hour (Fig. 4.16). The microstructure of the aged specimen shows that the acicular α has been destroyed and the transformed β-phase exists with minute α particles in a retained β-matrix after aging.

It is anticipated that the fracture strength of the aged diffusion welded specimen would be higher than that of the original diffusion welded specimen due to destruction of acicular α plate[47].

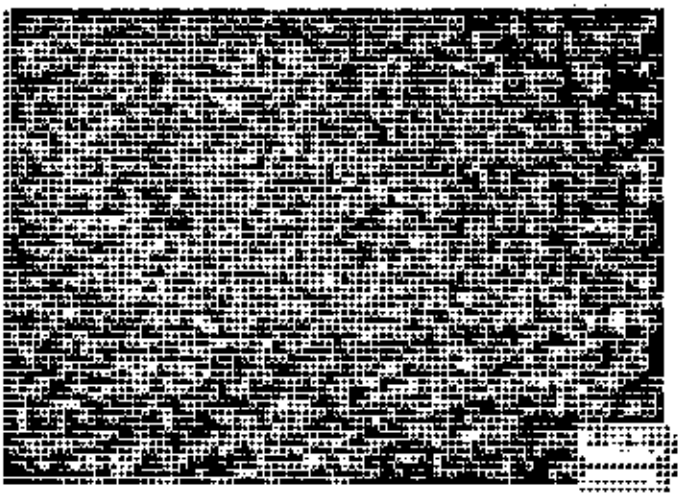

Figure- 4.1 The microstructure of the as received samples of IMI-325.

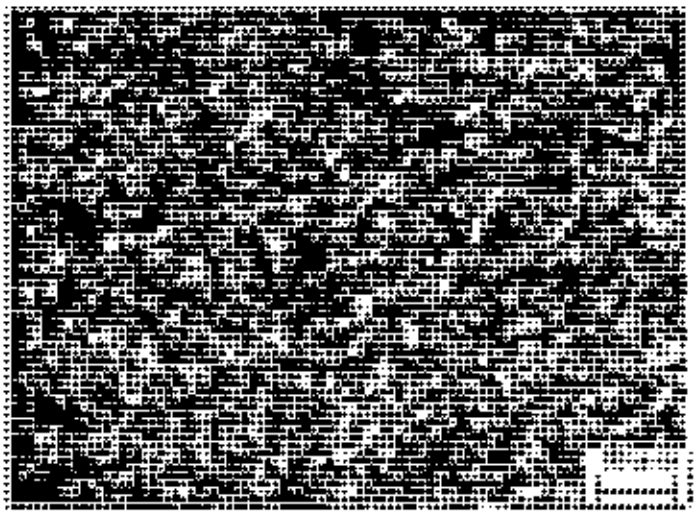

(a)

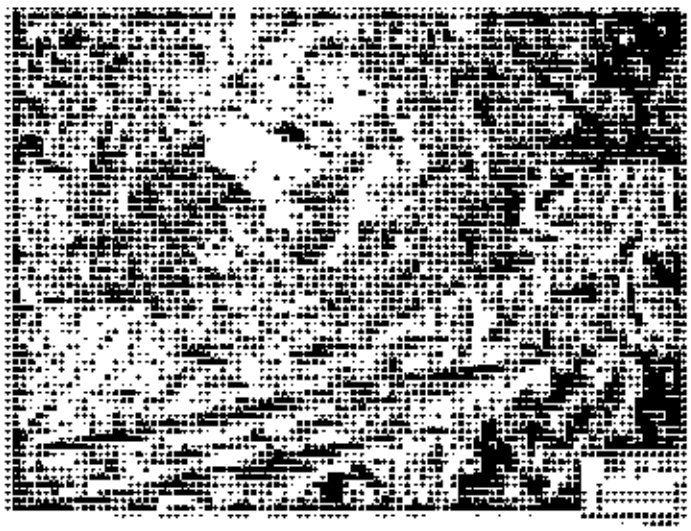

(b)

Figure 4.-2 The microstructures of water quenched IMI-325 showing the variation of α/β phase proportion at the temperature of (a) 840°C and (b) 910°C for 30 minutes.

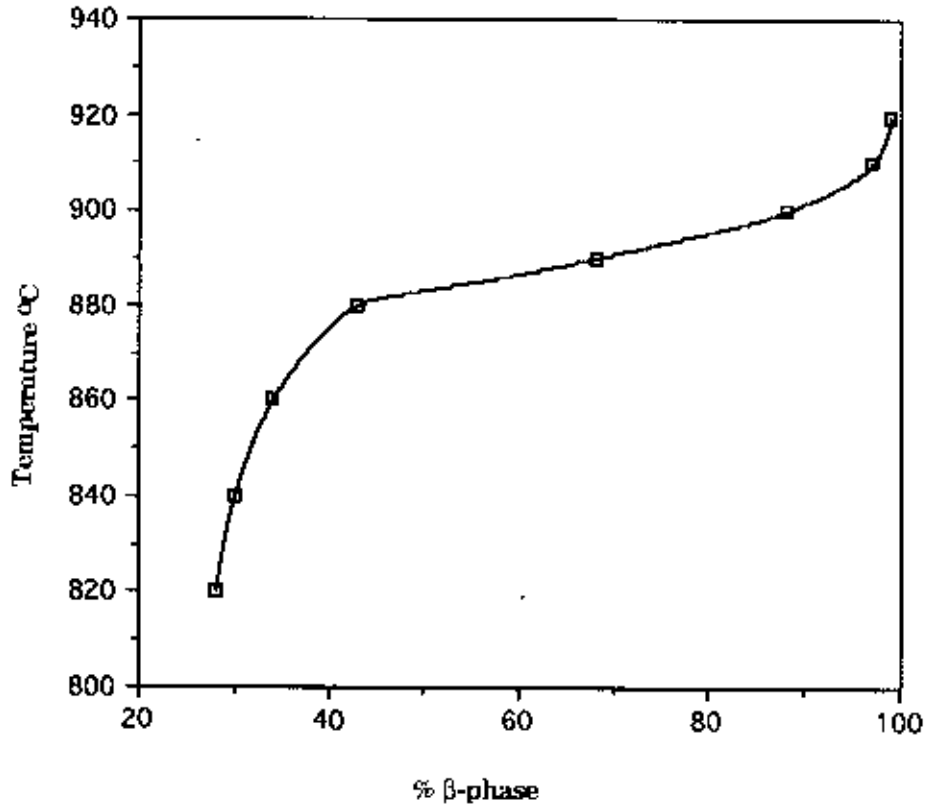

Figure- 4.3 Volume fraction of β phase versus temperature for IMI-325

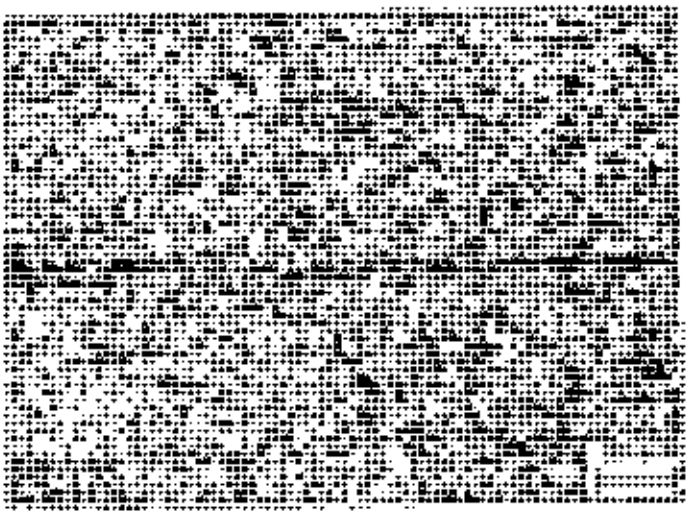

(a)

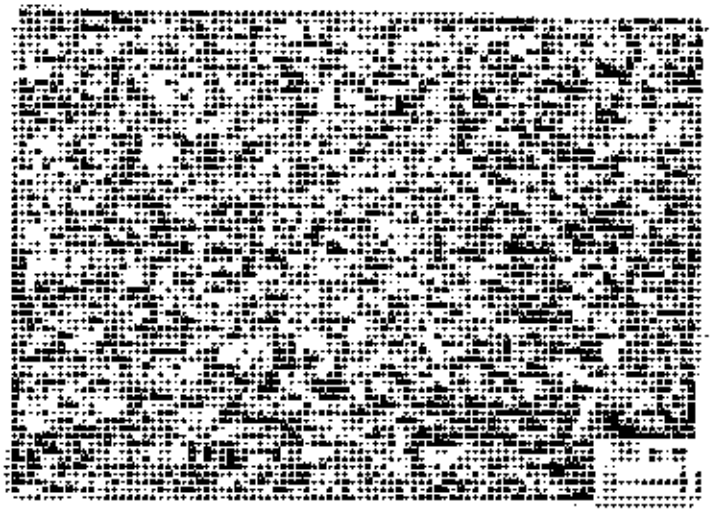

(b)

Figure 4.4 Microstructure of the diffusion weld in IMI-325 for 1 hour at (a) 840°C + 2.1 MPa and (b) 840°C + 2.5 MPa respectively.

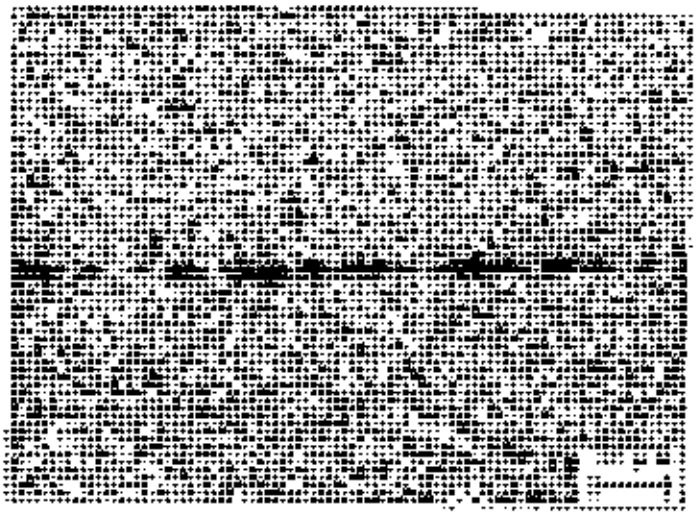

Figure-4.5 Microstructure of the interface between two sheet of IMI-325 with the applied pressure of 2.5 MPa (360Psi) at 860^{o}C for zero time.

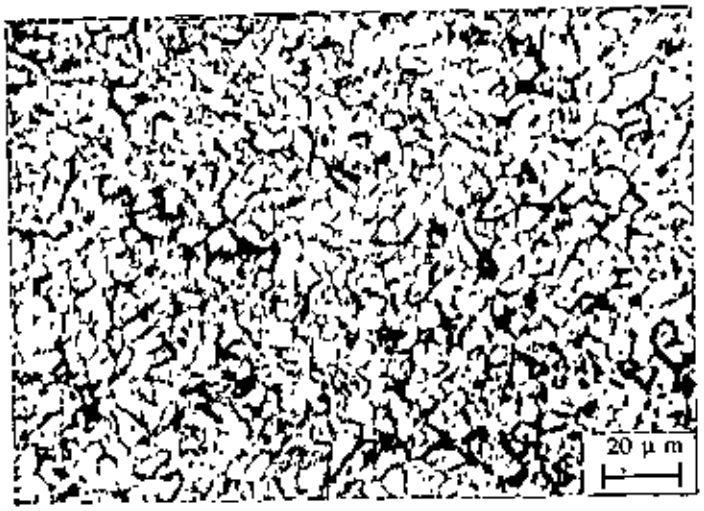

(a)

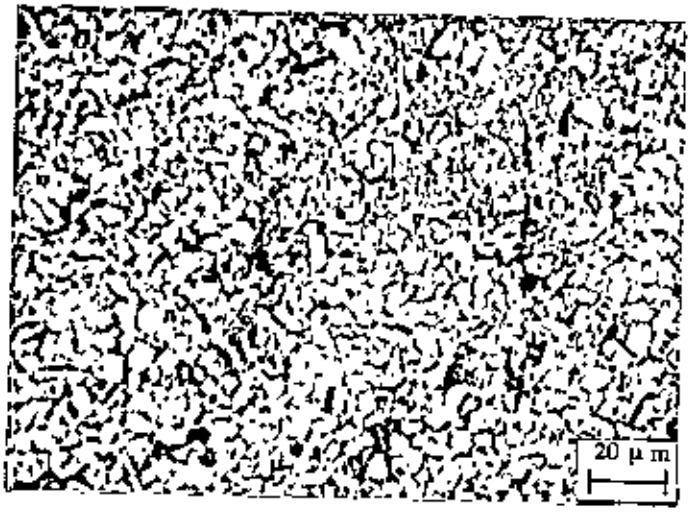

(b)

Figure 4.6 Microstructure of the diffusion weld in IMI-325 for 1 hour and at (a) 880°C and (b) 860°C respectively. The first one shows relatively larger grain due to the higher temperature

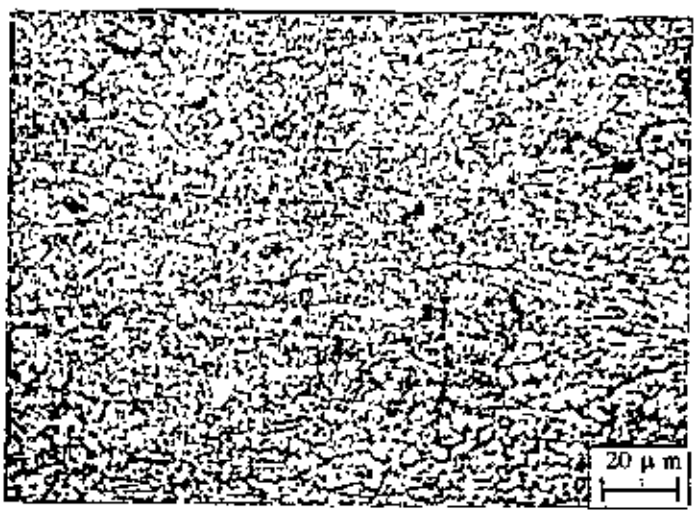

Figure- 4.7 The microstructure of the as received samples of IMI-318.

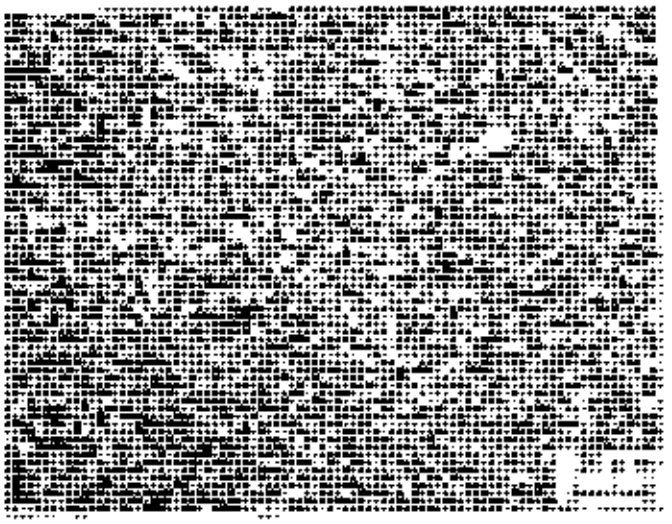

(a)

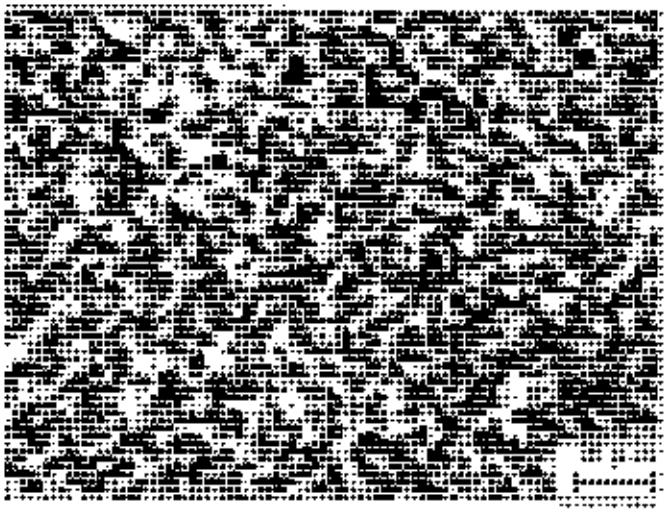

(b)

Figure- 4.8 Microstructures of the water quenched IMI-318 showing the variation of α/β phase at the temperature of (a) 880°C and (b) 940°C for holding time 30 minutes

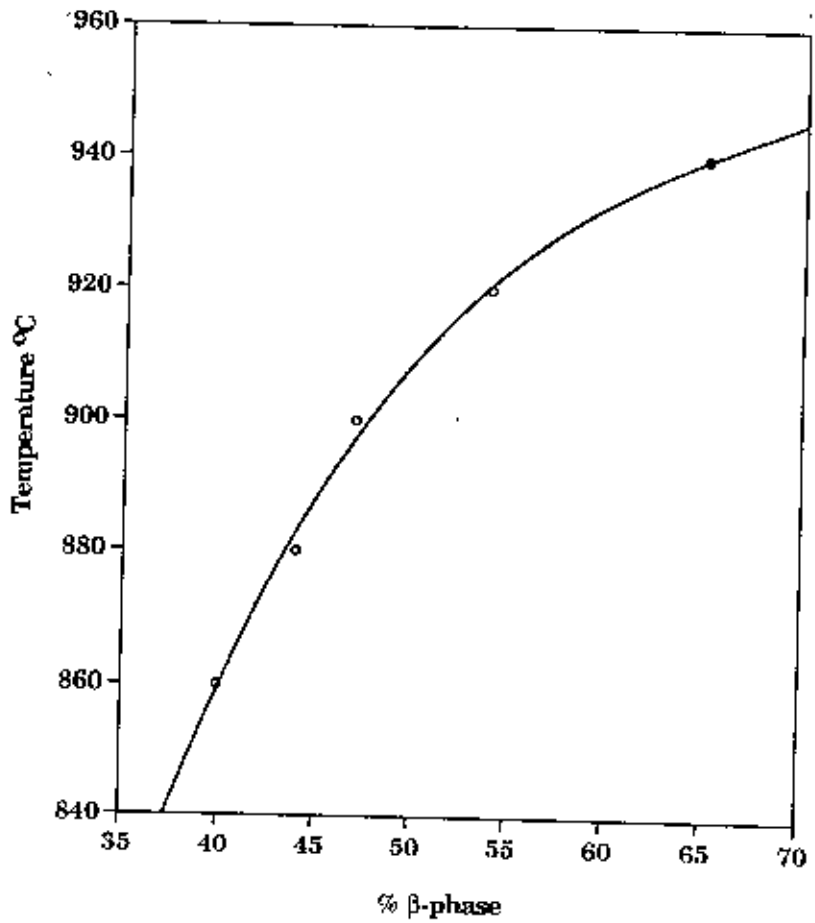

Figure- 4.9 - Volume fraction of β phase versus temperature for IMI-318

Figure 4.10 - Microstructure of the poor weld between IMI-325 to IMI-318 formed by using welding condition of 840°C + 2.1 MPa (300Psi)+ 1/2 hr.

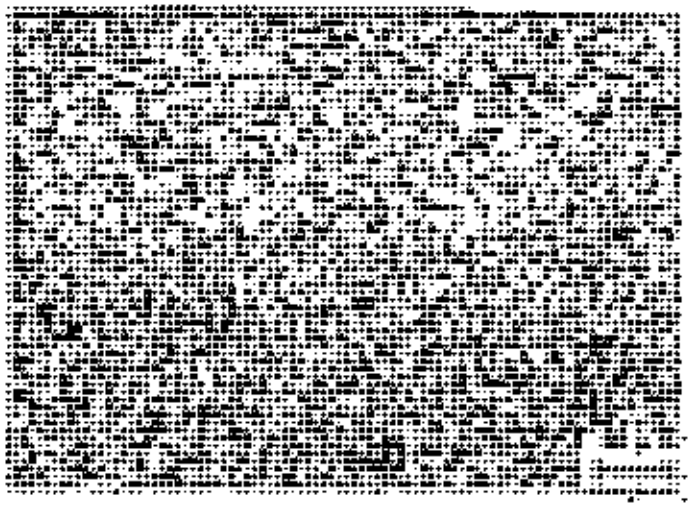

Figure 4.11 - Microstructure of the sound weld between IMI-325 to IMI-318 formed by using welding condition of 860°C + 2.1 MPa (300Psi)+ 1 hr.

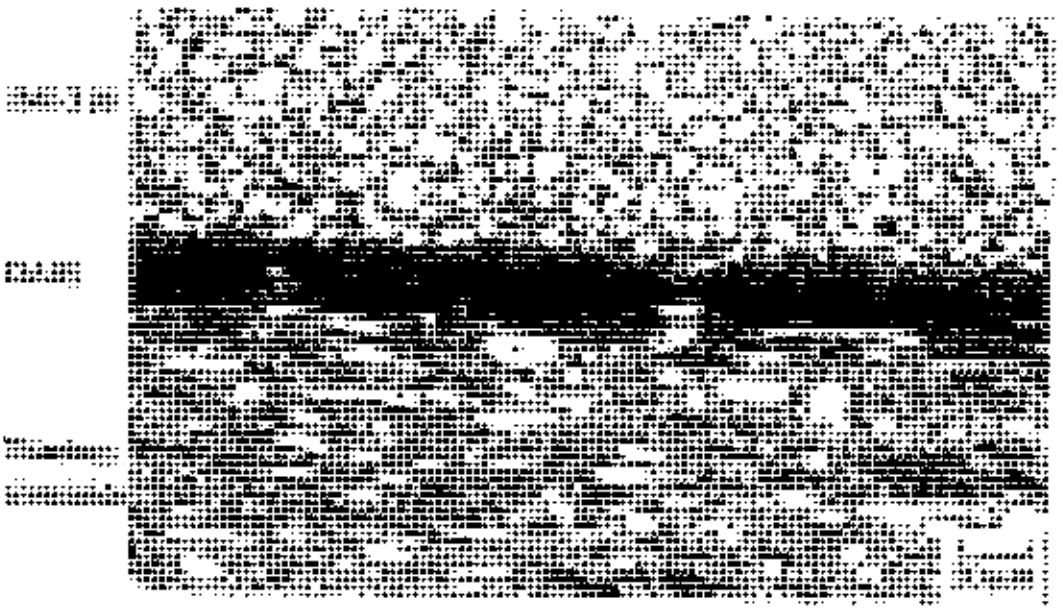

Figure 4.12 a - Microstructure of diffusion weld between IMI-318 to titanium aluminide using welding condition of 940°C + 10 MPa + 1 hr.

Figure 4.12 b - Microstructure of diffusion weld between IMI-318 to titanium aluminide using welding condition of 920°C + 10 MPa + 1 hr.

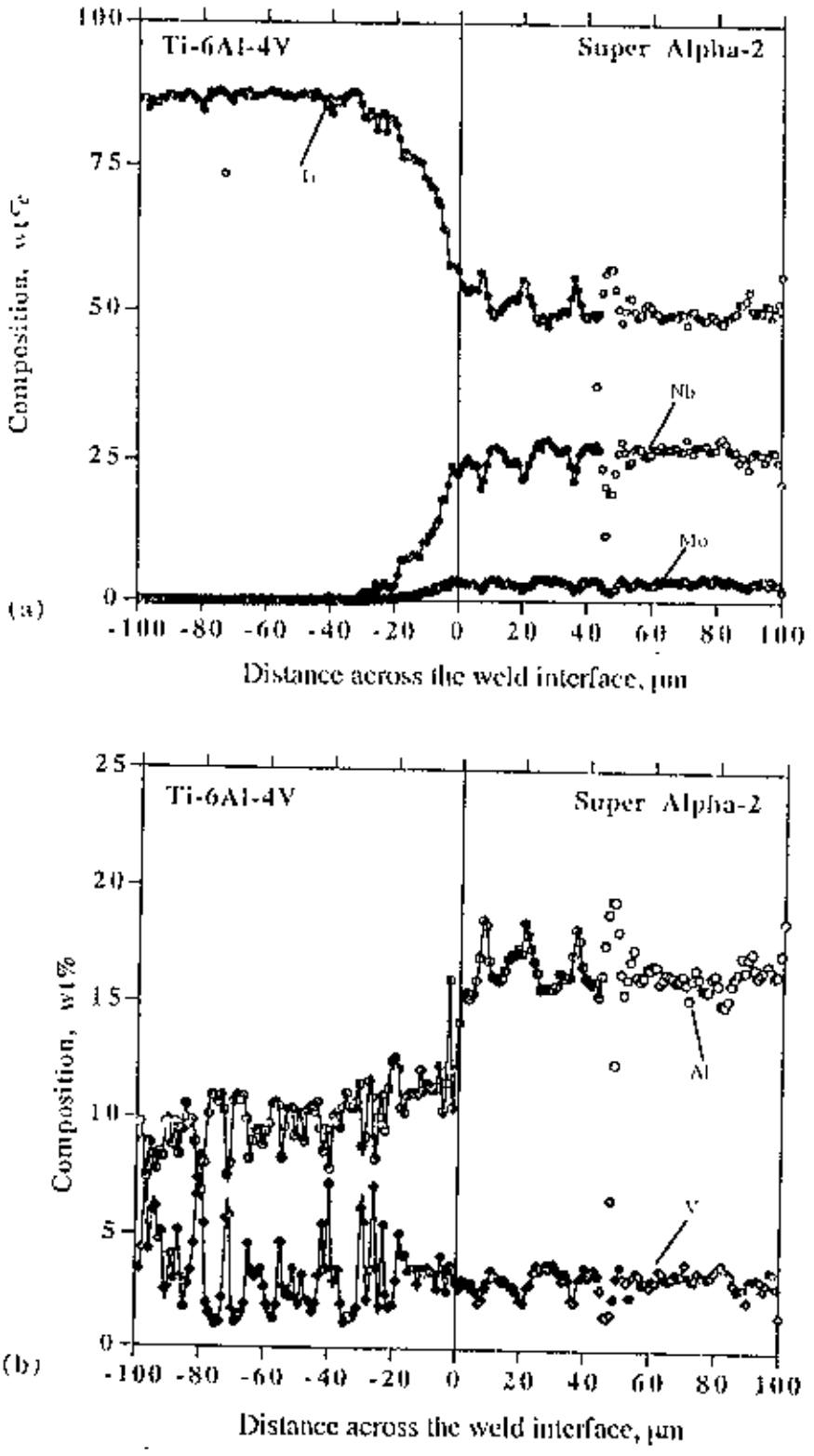

Figure 4.13 - Compositional profile across diffusion weld interface of the IMI-318 to titanium aluminide alloy; (a) Ti, Nb, and Mo (b) Al and V; weld condition : 940°C + 10 MPa + 1 hour.

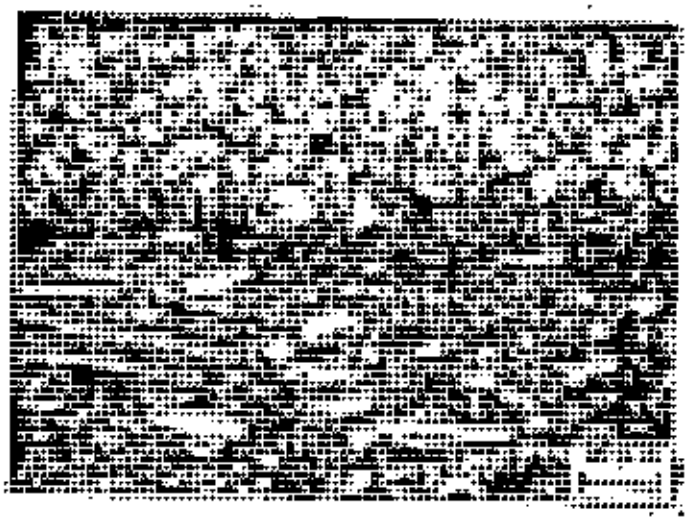

Figure 4.14 - Microstructure of the diffusion welded specimen (IMI-318 to titanium aluminide welded at 940°C + 10 MPa + 1 hour) which is solution-treated at 920°C for 1hour and furnace cooled.

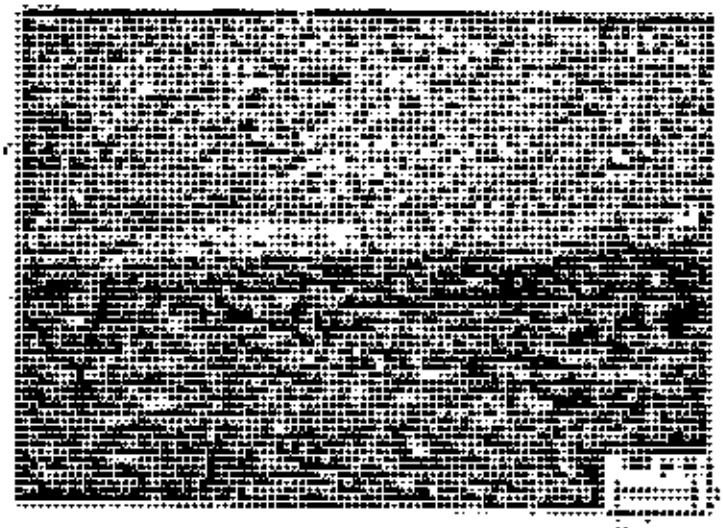

Figure 4.15 - Microstructure of the diffusion welded specimen (IMI-318 to titanium aluminide welded at 940°C + 10 MPa + 1 h) which is solution-treated at 900°C for 2h and water-quenched.

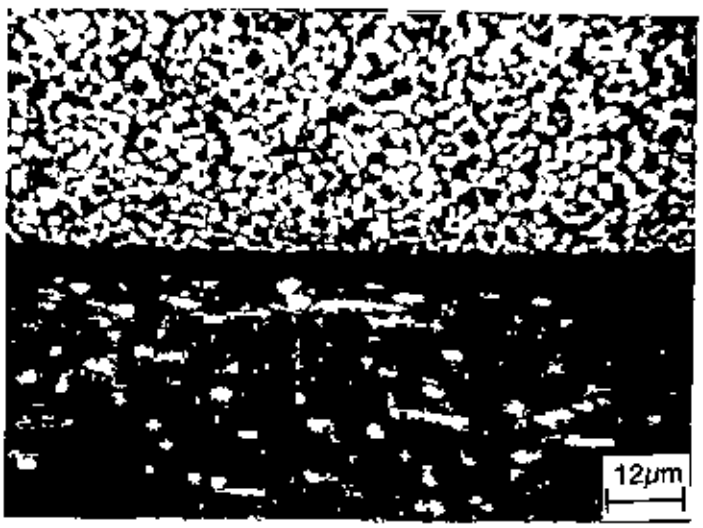

Figure 4.16 - Microstructure of the diffusion welded specimen (IMI-318 to titanium aluminide welded at 940°C + 10 MPa + 1 hour) which is solution-treated at 900°C for 2 hour, water-quenched and aged at 700°C for 5 hour.

CONCLUSION

1) A small vertical furnace has been constructed locally . Although it has been used to characterize Ti-alloys, it can also be used for other purpose such as the determination of TTT-diagram for a particular alloy.

2) 40-50% β phase exists in the range of 840°C-880°C for IMI-325 and 860°C-920°C for IMI-318. In these temperatures range the grain size was less than 10 μm for both the alloys. The β-transus temperature for IMI-325 has been found to be ~920°C.

3) A mini hot isostatic furnace has been developed which is a real achievement of the present work.

4) Sound weld has been found for both the similar IMI-325 and the dissimilar IMI-325 to IMI-318 at the condition of 860°C+2.1MPa+1hour.

5) Post heat treatments of the welded specimens of IMI-318 and titanium aluminide have destroyed the Widmanstätten α in the weld region forming finely distributed α phases in the transformed β matrix.

REFERENCES

1. J. Pilling J., Materials Science and Engineering, 1988, **100**, 137-144.

2. M. F. Islam, Ph. D. thesis, Materials Science Center, UMIST, England, 1995, 5-151.

3. J. Pilling and N. Redley `SUPERPLASTICITY - in crystalline solids' Institute of Metals, London ,1988, 159-195.

4. C.H. Hamilton, in Titanium Science and Technology, (ed R.I. Jaffee and R.M.Burte), Plenum, NewYork, 1973, 625.

5. H. V. Atkinson, and B. A. Rickinson; "Hot isostatic Processing", Adam Hilger, London, 1990, 1- 86.

6. A. S. Rao and C. D. Chaklader. J. Am. Ceram. Soc., 1972, **55**, 596.

7. D. S. Wilkinson and M. F. Ashby, Acta metall., 1975, **23**, 1277.

8. J. R. Matthews, Acta metall., 1980, **28**, 311.

9. E. Arzt, M. F. Ashby and K. E. Easterling, Metall. Trans., 1983, **14A**, 211.

10. F. B. Swinkels, D. S. Wilkinson, E. Arzt and M. F. Ashbey, Acta Metall., 1983, **31**, 1829-1840.

11. A.S. Helle, K.E. Easterling, and M.F. Ashby, Acta Metall., 1985, **33**, 2163-2174.

12. J. F. Lancaster, "The Metallugy of welding" George Allen and Unwin Ltd., London, 1980, 1-7.

13. Y. Machara, Y. Komizo, T. G. Longdon, Mat. Sci. Tech., 1988, 4, 669-674.

14. A. Hill, and E.R. Wallach, Acta Metall., 1989, **37**, 2425-2437.

15. G. Garmong, N. E. Paton and A.S. Argon, Metall. Trans., 1975, **A6**, 1269.

16. B. Derby and E.R. Wallach, Metal Sci., 1982, **16**, 49.

17. J. Pilling, D.W. Livesey, J.B. Hawkyard and N. Ridley, Metal. Sci., 1984, **18**, 117.

18. B. Derby and E.R. Wallach, Metal Sci., 1984, **18**, 427.

19. Z. X. Guo and N. Ridley, Mater. Sci. Technol., 1987, **3**, 945.

20. M. M. I. Ahammed and T. S. Langdon: Metall. Trans., 1977, **8A**, 1832-1833.

21. K. Higashi, T. Ohnishi, and Y. Nakatami: Scr. Metall., 1985, **22**, 821-824.

22. N. Ridly, Mat. Sci. Tech., 1990, **6**, 1145-1156.

23. T. G. Langdon: in `Superplastic forming of structural alloys', (ed. N. E. Paton and C. H. Hamilton), Warrendale, PA, The Metallurgical Society of AIME, 1982, 27-40.

24. H. T. Courtney, in "Mechanical behavior of Materials", Mac Grow-Hill Publishing Company, New York, 1990, 295-298.

25. J. A. Wert: in `Superplastic forming of structural alloys', (ed. N. E. Paton and C. H. Hamilton), Warrendale, PA, The Metallurgical Society of AIME, 1982, 69-83.

26. E. E. Underwood: J. Met., 1962, **14**, 914.

27. M. F. Islam, and N. Ridley, Hot Isostatic Pressing '93, (ed. Delacy D. and Tas, T.), 1994, 325-332.

28. E. D. Weisert and G. W. Stacher: in `Superplastic forming of structural alloys', (ed N. E. Paton and C. H. Hamilton), Warrendale, PA, The Metallurgical Society of AIME, 1982, 237-289.

29 J. R. Williamson: in `Superplastic forming of structural alloys', (ed. N. E. Paton and C. H. Hamilton), 27-40; 1982, Warrendale, PA, The Metallurgical Society of AIME.

30. D. Stemphen, "Designing with Titanium", Institute of Metals, London, 1986, 108-115.

31. Polmair, "Light Metals", Edward Arnold, London, 1988, 211-271.

32. Y. Lakhtin, "Engineering Physical Metallurgy and Heat-treatment", Mir publishers Moscow, 1985, 363-377.

33. S. H. Avner, "Introduction to Physical Metallurgy", MacGrow Hill Company, 1987, 524-530.

34. E. W. Collings, "The Physical Metallurgy of Titanium Alloys", ASM, Metals Park, OH, 1984, 116.

35. H. M. Flower, Met. Sci. Tech., 1990, **6**, 182-192.

36. D. Porter and K. Easterling, "Phase Transformation of metals and alloys", Chapman & Hall, London, 366-372.

37. D. Eylon, J. A. Hall, C. M. Pierce, and D. L. Ruckle: Metall. Trans. 1976, **7A**, 1817-1826,

38. S. R. Seagle and L. J. Bartlo: Met. Eng. Q., 1968, **8**, 1-10.

39. D. Eylon, C. M. Pierce, and J. A. Hall: Metall. Trans., 1976, **7A**, 111-121.

40. I. W. Hall and C. Hammond: in 'Titanium and titanium alloys, (ed. J. C. Williams and A. F. Belov), New York, Plenum Press, 1982, 601-613.

41. J. J. Lucas: in 'The titanium science and technology', (ed. R. I. Jafee and H. M. Burte), New York, Plenum Press, 1973, 2081-2095.

42. N. L. Richards and J. T. Barnby: Mater. Sci. Eng., 1976, **26**, 221-229.

43 P. J. Bania, L. R. Bidwell, J. A. Hall, D. Eylon, and A. K. Chakrabarti: in 'Titanium and titanium alloys,' (ed. J. C. Williams and A. F. Belov), New York, Plenum Press, 1982, 663-677.

44. S. L. Semiatin and G. D. Lahoti: Metall. Trans., 1981, **12a**, 1705- 1717.

45. M. F. Islam and M. O. Alam, "Interface Characteristics of Isostatic Diffusion Welding between Dissimilar Titanium Alloys", (To be Presented at Symposium on Extraction and Processing of Titanium, TMS Materials Week, Indianapolis, Indiana 14-18 September 1997).

46. M. C. Juhas et al., Titanium '92 - Science and Technology, (ed. Froes, F. H. and Caplan, I. L.,) TMS, 2, 1993, 1453-1460.

47. J. Pilling, M. F. Islam, and N. Ridley, Mat. Sci. Eng., 205, 1996, 72- 78.